Downscaling leaf area index using downscaling cokriging on optical remotely sensed data

ANKUR SINGH
March. 2013

ITC SUPERVISOR
Dr. N.A.S. Hamm

IIRS SUPERVISORS
Ms. Vandita Srivastava

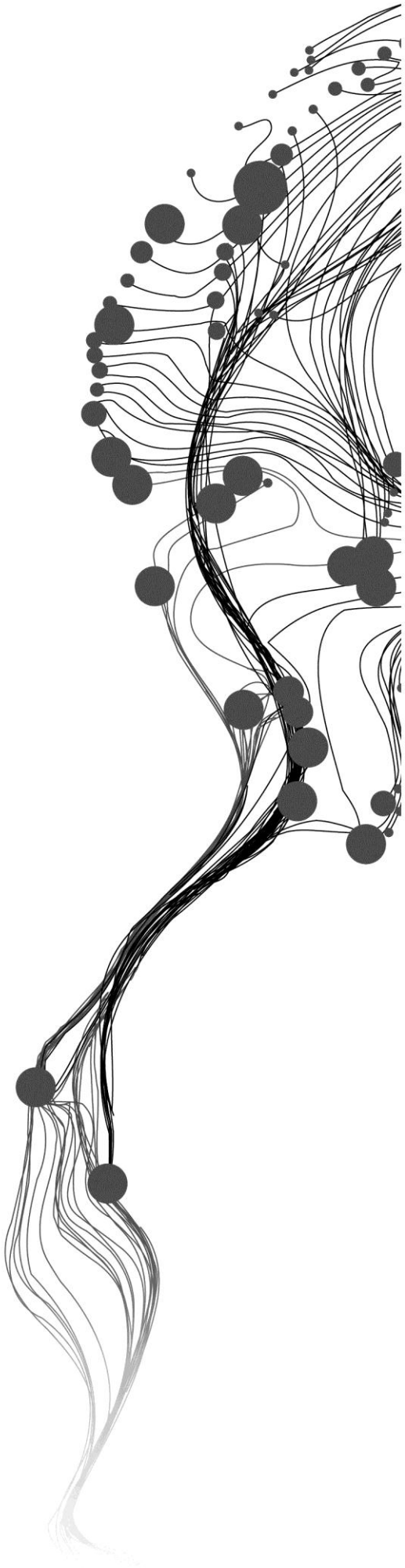

Downscaling leaf area index using downscaling cokriging on optical remotely sensed data

ANKUR SINGH
Enschede, the Netherlands [March, 2013]

Thesis submitted to the Faculty of Geo-information Science and Earth Observation of the University of Twente in partial fulfilment of the requirements for the degree of Master of Science in Geo-information Science and Earth Observation.
Specialization: Geoinformatics

ITC SUPERVISOR	**IIRS SUPERVISORS**
Dr. N.A.S. Hamm	Ms. Vandita Srivastava

THESIS ASSESSMENT BOARD:

Chairperson	: Prof.dr.ir. M.G. Vosselman
ITC Theme Leader	: Prof. dr.ir. A. Stein.
First Supervisor (IIRS)	: Ms. Vandita Srivastava
Second Supervisor (ITC)	: Dr. N.A.S. Hamm
External Examiner	: Prof C.Jeganathan(BIT,Ranchi)

Indian Institute of Remote Sensing
Indian Space Research Organisation
Department of Space, Government of India,
ISO 9001-2008 Certified

FACULTY OF GEO-INFORMATION SCIENCE AND EARTH OBSERVATION,
UNIVERSITY OF TWENTE,
ENSCHEDE, THE NETHERLANDS

DISCLAIMER

This document describes work undertaken as part of a programme of study at the Faculty of Geo-Information Science and Earth Observation (ITC), the University of Twente, The Netherlands. All views and opinions expressed therein remain the sole responsibility of the author, and do not necessarily represent those of the Faculty.

"The keys to patience are acceptance and faith. Accept things as they are, and look realistically at the world around you. Have faith in yourself and in the direction you have chosen."

By: **Ralph Marston**

-

Dedicated to my parents.....

ABSTRACT

In the field of remote sensing, scaling of data has become more practicing in different disciplines. Downscaling of data bring revolution for the usage of coarse spatial resolution data products. The data products were downscaled to desired fine resolution according to the usage. In this study LAI (leaf area index) is downscaled by using cokriging technique. The main aim of this research is to explore downscaling cokriging technique by studying the effect of resampling and point spread function (PSF).

MODIS LAI product at 1000 m spatial resolution is used as primary variable and MODIS NDVI at 250 m is used as covariable to downscale LAI at 250 m. Cokriging is used as the technique for downscaling. The first step for downscaling cokriging involves the calculating of sample variogram and cross-variogram. To calculate cross-variogram both the variable LAI and NDVI should be on same scale. To bring MODIS LAI at 250 m it is resample at 250 m and cross-variogram is calculated between resample LAI and original NDVI at constant cut-off of 6000 m and bin of 15 and variogram and cross-variogram is modelled at common range of 3817.4 m using exponential model. To select optimal resampling from different resampling techniques (nearest neighbour, bilinear interpolation, cubic convolution and trivial method) variogram analysis has been executed. It was found that variance in trivial resampling was highest (sill = 3.78) which shows high spatial dependence. Trivial resampling is also selected for resampling because it resample's pixel size with original pixel values. Gaussian and uniform PSF are used to study the effect of PSF on variogram. Standard deviation σ_x and σ_y were parameterized by experimenting with different value of standard deviation. σ_x and σ_y were parameterized at 250 m for MODIS LAI at resolution 1000 m and 122.5 m for MODIS NDVI at resolution 250m. Further, point support variogram and cross-variogram were estimated to see the effect of both (uniform and Gaussian) PSF by keeping rest of the parameter same and using nested exponential model. It was found that for LAI 1000 m using uniform PSF sill was 2.85 for the range 3040.5m which is more than that by using Gaussian PSF (2.06 for range 3857.0 m). It was found that variance is high using uniform PSF for LAI at 1000 m because distance from the pixel or the mean is more. It was observed that for NDVI at 250 m there is very less difference is observed by estimated point support variogram which was not observed by modelling of point support variogram in and variance for uniform PSF was found higher than by using Gaussian PSF. There was no change observed for the cross-variogram because PSF does not have much effect for different bands on same support. Due to above change the effect was also observed on the centre of downscaling cokriging weights. By using uniform PSF centre of the weight was high than that by using Gaussian PSF. There is change observed in the downscaled cokriging image. The downscaled image for Gaussian PSF was found smoother than that of uniform PSF. The standard deviation in downscaled image for uniform PSF (1.73) was found more than that of Gaussian PSF (1.69) which shows that variance is high for the uniform PSF than that of Gaussian PSF.

Keywords: Downscaling, cokriging, MODIS LAI, MODIS NDVI, resampling, Point spread function (PSF), uniform PSF, Gaussian PSF, variogram

ACKNOWLEDGEMENTS

This thesis duration is one of the most learning phases of my life. The modules and pilot projects during my M.Sc. course became the base of this research. I would not have finished this research successfully without the help, support and moral boosting from many individuals.

Firstly and most importantly I would like to show my gratitude toward my supervisors Ms. Vandita Srivastava and Dr. Nicholas Hamm. Their expert guidance, valuable suggestions, constructive criticism and encouragement act as a four pillar of my thesis. Their critical and logical thinking helped me to complete this thesis successfully. Thanks to you both.

I would like to show honour to Prof. Alfred Stein and Dr. Nicholas Hamm for givng a valueable lecture in ITC on geostatistics which make my interest in the subject and also providing all small details on formalizing MSc thesis on their last visit to IIRS.

I would also like to acknowledge Mr. Prasun Kumar Gupta GID, IIRS who had spent his valuable time to help me out with the FORTRAN software issues.

I would also like to thank IIRS-ITC joint education program for allowing me to get into M.Sc. course. This course taught me a lot academically and also helped me to explore the culture of The Netherlands. I am also thankful to ITC for providing access to excellent facilities like electronic library, blackboard, webmail, softwares etc.

I would also like to give special thanks to Dr. Y.V.N.Krishna Murthy, Director IIRS, Mr. P.L.N. Raju, Group head (RS and GIS) IIRS and Dr.S.K.Srivastava, Head Geo Informatics Division, IIRS for providing wonderful infrastructure which has helped me in finishing this research successfully and taking care of all the requirements. I am also thankful to IIRS library and CMA department for providing me facilities and resources.

I specially thank Priyanka Arya, for her keen support to keep my moral high and helped to stay focused on my project. I am also thankful to my roommate and friend Jayson for his outstanding support and for many fruitful discussions which helped in expanding my knowledge.

I would also like to thanks all my friends in IIRS and outside IIRS for their support and for the wonderful time spent here.

Last but not the least, without the support of my family and almighty god I would not have finished this project. Since, they were not present here with me but their blessings and support was always to my take care.

TABLE OF CONTENTS

LIST OF FIGURES

LIST OF TABLES

1. INTRODUCTION

1.1. Background

In the field of remote sensing, scaling of data has become more practicing. According to the application, the resolution of the data can be changed either by upscaling or downscaling. Upscaling refers to the practice of converting finer spatial resolution data to coarser spatial resolution data. For example, ground data are upscaled to match with the pixel of an image (Atkinson, 2012). Downscaling is when coarser spatial resolution is converted to finer spatial resolution. These days' downscaling is of much interest to the researchers for exploration and to practitioners for implementing the fusion of different data of varying scales. The reason an optimal pixel size is defined by researchers is due to the issue of scaling (Atkinson and Curran, 1995; Atkinson et al., 1997; Woodcock and Strahler, 1987). The sensor which has the coarse resolution has a large coverage and high revisit time, which provides ample information more frequently. For example, MODIS has a spatial resolution of 250 m, 500 m and 1000 m and has a revisit time of more than 8 days. On the other hand, fine spatial resolution gives more detailed information with low revisit time. For example ASTER and LANDSAT series satellite has revisit time of 16 and 18 days.

The advantage of downscaling is to extract the detailed information from coarser resolution at high temporal resolution. This technique is also cost effective since fine resolution data are costlier than coarse resolution data. Atkinson (2012) stated that there are two approaches for downscaling: regression approaches and area to point predictions. In regression approach, finer spatial resolution is estimated from a coarser spatial resolution. This is done with the help of covariate as a variable. This approach does not consider support and also does not characterize pattern of spatial variation while area to point prediction interpolates using both support and also characterizes the pattern of spatial variation (Atkinson, 2012). In the present study, area to point prediction is used as technique, leaf area index (LAI) is used as a target or primary variable and NDVI is used as a covariable for downscaling.

Leaf area index is one of the main variables for characterizing plants' canopy. Leaf area index (LAI) is defined as the area of one side of the leaf per unit area of the ground (Myneni et al., 2002) It is a biophysical variable which influences vegetation photosynthesis, transpiration and land surface energy (Tian et al., 2002). It is an important variable of ecosystem because most of the ecosystem models that stimulate carbon and hydrological cycles require LAI as an input (Gower et al., 1999). Estimating LAI has become easier by using satellite data like MODIS which has a LAI product of spatial resolution of 1000 m for every 8 days. Much research has been conducted to estimate LAI for different forest types like coniferous forest, tropical forest, deciduous forest and broadleaf forest (Asner et al., 2003)

Earlier estimating LAI was a tedious task and usually unhelpful because the scientists needed to cut the plants from the soil surface, separate leaves from other part of the plant and measure individual leaf area to obtain the average leaf area per plant (Wilhelm et al., 2000). There are two methods to estimate LAI i.e. direct and indirect method. Direct methods are destructive method and time consuming. Indirect methods are constructive methods and are faster than the destructive methods. Indirect methods measure the light transmission through plant canopies using various instruments such as the Ceptometer, LiCor LAI-2000, hemispherical photography, etc.(Chen and Leblanc, 1997; Fassnacht et al., 1994; Wang et al., 2005).

Several studies have been conducted to estimate LAI by using vegetation indices (Hwang et al., 2011). Due to presence of chlorophyll in the leaves, it absorbs blue and red radiations and scatter near infra-red (NIR) radiation so vegetation indexes are used to estimate LAI. In remote sensing, NDVI has been usually used to estimate LAI because of its relationship with LAI (Miller et al., 1997; Spanner et al., 1990). The phenological changes in LAI are related to NDVI which varies every year and in every season and it depends on the growth of the trees. Myneni et al. (2002) used NDVI to estimate LAI/FPAR from the MODIS (Moderate resolution imaging spectroradiometer) sensor at a coarse spatial resolution of 1000 m.

In this research area to point prediction (prediction of continous variable through prediction) approach is used to downscale and cokriging is used as a predictor. In cokriging one or more co-variables are require for downscaling. These covariable must be highly correlated with primary or target variable. This approach involves estimating two variograms of primary and secondary variable and cross-variogram between resample primary variable and original covariable on the point support. Cokriging is an unbiased predictor and minimizes prediction variance. In cokriging linear system of theory is used to define the different supports for same variable (Pardo-Iguzquiza and Atkinson, 2007). In this study effect of uniform point spread function and Gaussian point spread function are studied. The point spread function is used to build a theoretical relation between semi-variogram and cross-variogram. "*Cokriging system involve estimation of linear model of co regionalization of point support covariance and cross-covariance by numerical de-convolution and predict the target image by convolution*" Pg (91) (Pardo-Iguzquiza et al., 2006) .

In this study, effort is made to downscale LAI from 1000 m spatial resolution to 250 m spatial resolution by using cokriging and also study the effect of resampling and PSF on the downscaling cokriging. In this study downscaling cokriging is performed by using uniform and Gaussian PSF and to study its effect on the downscaling cokriging which is also an innovation of this project. It will also help to monitor vegetation for heterogeneous forest at finer scale. Coarser resolution imagery covers a large area due to which it loses important spatial structure, topographic variance and vegetation patterns (Hwang et al., 2011). So at this resolution it is not sufficient to estimate LAI for specific purpose like for monitoring heterogeneous forests. Downscaling of this coarser data will resolve this problem. It will be helpful for forest resource department to monitor vegetation at finer scale. It will also help to estimate LAI where field is not possible.

1.2. Research Identifications

1.2.1. Research Objectives

The main objective of this research is to study the effect of resampling and PSF on downscaling cokriging technique for LAI estimation.

Sub-objectives:

1. To downscale LAI using cokriging by covariable.
2. To study the effect of resampling on variogram.
3. To study the effect of PSF on variogram and downscaled LAI image.

1.2.2. Research Questions

To achieve the above objective the following questions need to be answered.

1. What is the suitable covariable and its correlation with LAI?
2. What is the effect of resampling on variogram and cross-variogram?
3. What is the effect of PSF on variogram and cross-variogram?
4. What is the effect of PSF on resultant downscaled image?

1.3. Innovation aimed at

The innovation of this project is to perform downscaling cokriging by using uniform and Gaussian PSF and also to study the effect of these PSF on downscaling cokriging technique.

1.4. Thesis Strucure

This structure of the thesis describes the whole project and the content related to this research in chapters:

Chapter 1: Introduction, this section describes general overview about this research work. It describe the basic idea of topic, motivation for selecting this topic, problem statement, research objectives, and research questions to carry out this task.

Chapter 2: Theoretical Background and Literature Review, this chapter contains theoretical background of the study and literature study.

Chapter 3: Study area and data used, this chapter describes selection of study area and description of the study area. It also contains the description of data used and software used.

Chapter 4: Methodology, this chapter describes complete workflow of the study and description of each and every steps of methodology.

Chapter 5: Results, this chapter contains results which I obtained using above methodology.

Chapter 6: Discussion, this chapter explain results and also its implications.

Chapter 7: Conclusion and Recommendation, this section describes the answer of the research questions in conclude form. Some important points are recommended after experience got from this whole work and recommendation for future work.

2. CONCEPTUAL AND THEORETICAL BACKGROUND

2.1. Terrestrial ecosystem

Terrestrial ecosystem has an essential role in the overall carbon cycle. It is responsible for the exchange of CO_2 which brings changes in atmospheric concentration. Terrestrial ecosystem affects the climate in number of ways that act over extent and duration scales. Forests are the most resourceful terrestrial ecosystem on Earth, providing essential goods and services upon which the humanity is very much dependent (Song, 2013). Due to changes in the area and changes during time in forest ecosystem affect global carbon cycle and also responsible for the climate change (Goodale et al., 2002). Increase in carbon content in forest ecosystems is a forewarning to take the most important step against global warming. Satellite remote sensing provides a unique way to obtain the distributions of LAI over large areas.

Leaf area index (LAI) is generally used to describe the photosynthetic and transpirational surface of plant canopies. LAI can be defined as the leaf surface area per unit ground area. It is an important variable in controlling many biological and physical processes. (Running et al., 1999) LAI is an essential input variable which is used for many climate and ecological models.

Green leaves are good absorbers of solar radiation. Compared with non vegetative surfaces, absorption in green leaves are more in visible spectrum for photosynthesis and less in near infrared radiation. Reflectance in red and near infrared wavebands has been used to formulate various vegetation indices because they indicate all the conditions of the vegetation surface (Qi et al., 1994). Among the various vegetation indices, NDVI (Wang et al., 2005), is most frequently used to derive LAI . There have also been several investigations on this relationship between satellite-derived vegetation indices and LAI for various forest type and species (Spanner et al., 1990(b); Spanner et al., 1990(a)).

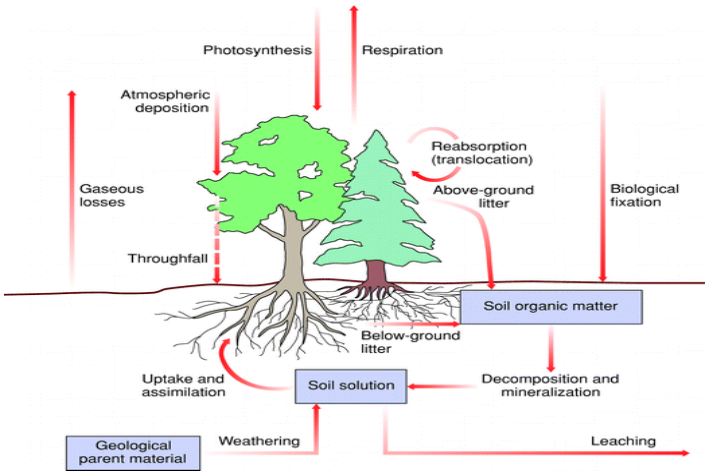

Figure 2-1 : Terrestrial ecosystem (Ollinger, 2003)

2.2. Biophysical variables

2.2.1. Leaf Area Index

Leaf area index is most important biophysical variable of ecosystem models (Propastin and Erasmi, 2010). Spatial distribution of LAI on Earth's surface is helpful in understanding various biophysical processes within a terrestrial ecosystem, such as photosynthesis, respiration, transpiration, carbon and nutrient cycle and rainfall interception ((Fassnacht et al., 1997; Hu et al., 2003; Miller et al., 1997); Peng et al. (2003)). LAI describes physiological, climatological and biogeochemical conditions due to vegetation conditions (Asner et al., 1998). Asner et al. (2003) stated that LAI can be estimated, modelled, and analysed at different resolution scales (from a small tree to whole forest and from whole forest to whole continents level because it has no unit). LAI is strongly correlated to vegetation species, growing stage, seasonal variance, field conditions and management practices.

To estimate LAI many methods were used from several years. Jonckheere et al. (2004) describes different methods to estimate LAI which are categorized into 2 categories i.e.:

- Direct method
- Indirect method

The accuracy of direct method is more than that of indirect method because leaves are cut and measured manually. The main disadvantage of this method is that it is time consuming and for large scale it is not feasible. There is more error in this method because of repeating measurements. This method is further divided into sub categories i.e.:

- Harvesting and non-harvesting methods(which is well explained in (Jonckheere et al., 2004))
- Leaf area determination techniques (which is well explained in (Jonckheere et al., 2004))

Indirect methods are faster than direct method. In this method leaf area can be determined by another variable. Jonckheere et al. (2004) stated that in field, indirect method is subdivided into two categories i.e.

- Estimating LAI from indirect contact.
  - Inclined point quadrant
  - Allometric method
- Estimating LAI from indirect non-contact (optical method).
  - Digital plant canopy imager
  - Plant canopy analyzer
  - TRAC
  - Hemi-view

2.3. Vegetation Indices

Vegetation indices were developed to study the qualitative and quantitative coverage of vegetation by using remote sensing techniques (optical). Bannari et al. (1995) explained that spectral response of vegetation is the collection of vegetation type, soil reflection, environment effects, shadow, soil color, and moisture. Vegetation indices were developed to decrease the above effects and enhance vegetation response. Qi et al. (1994) stated vegetation indices and band ratio were developed to estimate more information on vegetation and its structure (i.e. canopy geometry, architecture, and health) by using two or more than two spectral bands of electromagnetic spectrum and which is not possible by using single spectral band. Simple ratio (SR) and normalized difference vegetation index (NDVI) are the most common vegetation indices to estimate LAI and other surface parameters from space-borne and air-borne remote sensing (Rouse J.W., 1974).

NDVI has an important role in remote sensing to study the spatial structure of vegetation. Its value ranges between -1 to +1. -1 represent that there is no vegetation and +1 represents the presence of dense vegetation and zero shows the barren land. Baret and Guyot (1991) stated that NDVI is highly related to ecological parameters, carbon dioxide, LAI, photosynthesis and NPP (net primary productivity). It enhances the contrast between soil and vegetation and minimizes the illumination conditions. NDVI is the ration of red and NIR reflectance and expressed as:

$$\text{NDVI} = \frac{\rho_{NIR} - \rho_R}{\rho_{NIR} + \rho_R} \qquad \text{Equation 2.1}$$

ρ_{NIR} is the reflectance in the NIR spectral band

ρ_R is the reflectance in the Red spectral band

2.4. LAI-NDVI relationship

Leaves reflect strongly in near-infrared region and weakly in blue and red band due to absorption. Thus LAI has positive relation with near-infrared reflectance and negative relation with red reflectance. The ratio of red to near-infrared reflectance is used to express the increasing difference between red and near-infrared reflection with increasing LAI (Curran, 1980). Maki et al. (2005) studied the relationship between LAI and NDVI using MODIS LAI product. In this study to understand the relationship between NDVI and LAI, NDVI was calculated by scattering from arbitrarily inclined leaves (SAIL) radiative transfer model and LAI was evaluated. That led to two results: (a) plant affected the canopy level NDVI during leaf expansion and leaf senescence periods, and (b) the relationships between NDVI and LAI of summer and that of autumn are different because of discoloration of the leaf during leaf senescent period. These results indicate that it is necessary to take into account the influence of the understory plant for estimating canopy LAI from NDVI during leaf expansion and leaf senescent periods, and it is also necessary to consider discoloration of the leaf during leaf senescent period.

Wang et al. (2005) explains the relationship between NDVI and LAI to the year 1996 to 2001 at a deciduous forest site. The NDVI–LAI relationship can vary both seasonally and inter-annually in respect of the variations in phenological development of the trees and in response to temporal variations of environmental conditions. Strong linear relationships are obtained during the leaf production and leaf senescence periods for all years, but the relationship is poor during periods of maximum LAI. The relationship is also affected by background NDVI, but this could be minimized by applying relative NDVI. Comparisons between AVHRR and VEGETATION NDVI revealed that these two had good linear relationships (R2=0.74 for 1998 and 0.63 for 2000). However, VEGETATION NDVI data series had some unreasonably high values during beginning and end of each year. MODIS enhanced vegetation index (EVI) was the only index that exhibited a poor linear relationship with LAI during the leaf senescence period in year 2001. Finally it was concluded that the relationship established between the LAI and NDVI in a particular year may not be applicable in other years, so attention must be paid to the temporal scale when applying an NDVI–LAI relationships. The LAI NDVI relationship is used in this study to downscale LAI. Downscaling is also termed as disaggregation and also like a resample image at desired pixel size but downscaling is not exactly a resampling.

2.5. Resampling

Image resampling is the technique to interpolate new pixel value's from the original pixel value when image is modified in term of row and column (Wade and Sommer 2006). Reduction and enlargement of the images causes change in pixel value but the extent of an image remain unchanged. The resampling effects are the real concern in image processing regarding its image quality. The quality is defined good when the interpolation of a new pixel value must be closer to original pixel value (Studley and Weber, 2010). There are three techniques for resampling i.e.

- Nearest neighbor
- Bilinear interpolation
- Cubic convolution

Nearest neighbour resampling technique is more popular in remote sensing. This technique uses the same nearest original pixel value to the new pixel value of the interpolated image. This technique does not changes or modify its pixel value (Baboo and Devi, 2010). The main advantage of this technique is that it is simple, implementation speed is high and original value does not change. The disadvantage of this technique is that it causes positional error along linear features. This positional error is due to realignment of pixels (eXtension, 2008). In the figure below the orange dot is the original value of the pixel and the red dot is the new pixel value. This new pixel is interpolated by the nearest orange dot without changing its value.

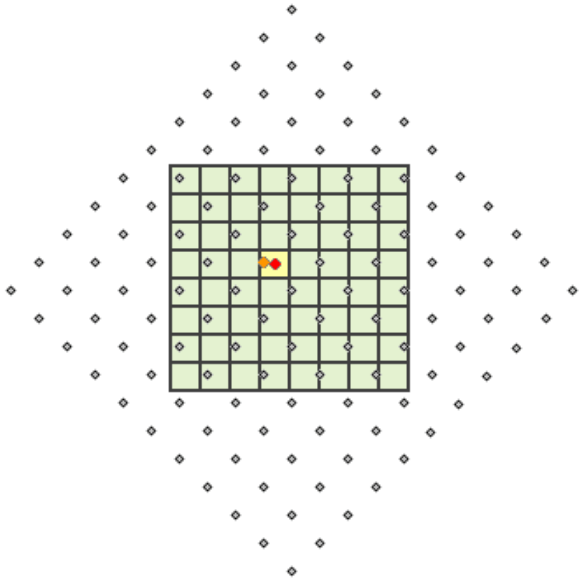

Figure 2-2 : Nearest Neighbour resampling (Studley and Weber, 2010)

Bilinear Interpolation is a technique where weighted average of the four nearest pixels is considered to interpolate a new pixel value in the resample image. This technique creates a new value to a pixel rather providing the same pixel value. Goldsmith (2009) stated that bilinear interpolation smoother the image and also produces better positional accuracy. The disadvantage of this technique is that it changes original pixel value and introduces a new pixel value which may not be present in the image. The figure below explains the bilinear interpolation.

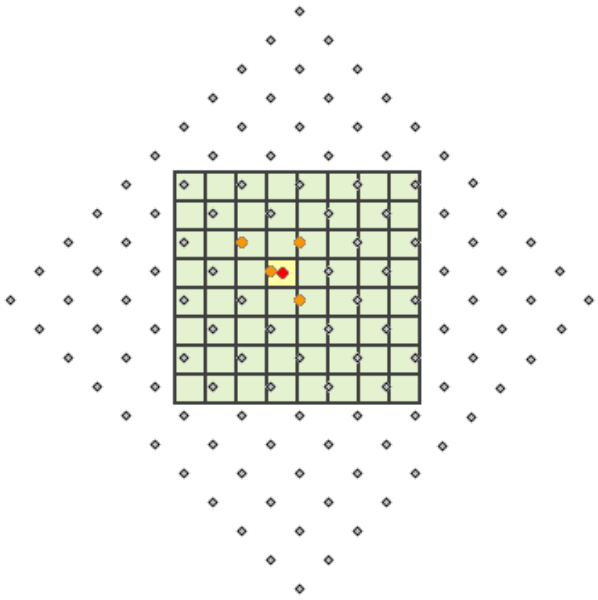

Figure 2-3 : Bilinear Interpolation resampling (Studley and Weber, 2010)

Cubic convolution is the technique which estimates a new pixel value by calculating the distance weighted average of sixteen nearest pixel. This method smoother images more than the bilinear and nearest neighbour resampling techniques. The main disadvantage of this technique is that it takes 10 to 12 times longer processing time than nearest neighbour (eXtension, 2008). The figure below explains cubic convolution method.

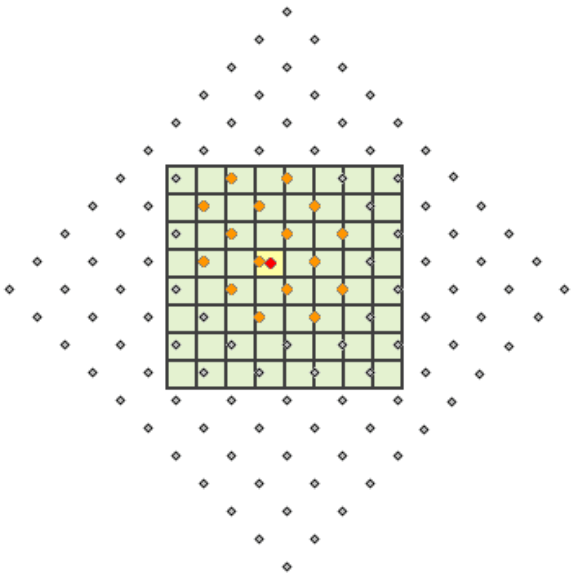

Figure 2-4 : Cubic convolution resampling (Studley and Weber, 2010)

2.6. Downscaling

2.6.1. Introduction

In remote sensing, sensors and geophysical surveys are important sources of information about the Earth surface and its properties. There are many satellite sensors of different spatial, spectral, and temporal resolutions. The spectral resolution is the band in electromagnetic spectrum like Landsat spectral resolution has seven bands and hyper spectral sensor has more than 100 bands so spectral resolution of hyper spectral is more than that of Landsat.

Satellite sensors which have coarse spatial resolution also had multiple classes within one pixel. Spectral un-mixing is the solution to determine the fraction of each class present in coarse pixel. The disadvantage of spectral un-mixing is that it yields only the fraction but does not locate them.

In this study LAI is downscaled. LAI product is available at a coarser resolution (> 1 km) at high temporal resolution. So there is always a question what should be the spatial resolution of LAI needed for the specific application (like monitoring vegetation, transpirational and photo-synthetically process of particular forest, etc.). LAI is important for many applications (like climate modelling, ecosystem modelling, vegetation dynamics, etc) directly or indirectly. Pandya et al. (2006b) suggested that for agricultural purpose LAI is needed at the fine resolution. For this purpose MODIS LAI product is not suitable because of its coarse spatial resolution. However the LAI product is available in coarse resolution but for fine resolution product is not available. Downscaling is one of the methods to retrieve fine spatial resolution LAI product. Downscaling is to convert coarse spatial resolution to fine spatial resolution as given in figure 2. Mustafa et al. (2011) stated that for validation of coarse resolution accurate high resolution LAI data is required and also he stated that there are uncertainties present in coarse resolution data.

2.6.2. Downscaling Techniques

There are several techniques available to estimate LAI from optical data. Atkinson (2012) explained that two downscaling techniques i.e. regression approaches and area to point prediction. Regression approach estimates finer resolution imagery with the help of covariate without considering the support. This method does not use the support effect and also does not characterize spatial variation trend of finer image. This method was developed by (Stathopoulou and Cartalis, 2009) to downscale AVHRR LST (land surface temperature) of 1 km resolution to Landsat TM band 6 of 120 m spatial resolution. They conducted this study using four case methods of scaling factor for downscaling. These scaling factors were TM effective emissivity, TM LST, combined use of TM LST and TM effective emissivity and use of high resolution estimate of AVHRR LST. They found that AVHRR LST show a optimal result with original generated LST value at 120 m. Pouteau et al. (2011) downscale MODIS 1 km resolution to 100 m by multiple regression and boosted regression tree (BRT) approaches. They used BRT model to downscale regional frost occurrence map for agriculture and land resource management. They also used a correlation between night land surface temperature and minimum air temperature for downscaling. Zhan et al. (2011) developed a method comprises regression approach with modulation approach. Kustas et al. (2003) developed TsHARP model based on inverse linear relationship between fine resolution NDVI and coarse resolution LST and Jeganathan et al. (2011) also developed TsHARP model by localizing the model fitting. Zurita-Milla et al. (2009) used spectral mixture analysis on multi-temporal images to downscale 300 m to 25 m resolution using categorical data.

In the above downscaling technique they did not consider support of the data. Area to point prediction used interpolation technique to downscale the coarse resolution as input variable into a same variable as a fine resolution variable. It considers the support of the data i.e. pixel support or point support of the data. Area to point kriging predicts on the support which is smaller than the original data.

Pardo-Iguzquiza et al. (2006) developed a downscaling technique using cokriging as predictor which is multivariate alternative to area to point kriging. They use ETM+ image for downscaling. This technique was developed for general application not for specific application. Cokriging is used in this technique because it is unbiased predictor. It involves two or more than two variables. It also minimizes the prediction variance and takes account of pixel support, point spread function (PSF) of the sensor, spatial correlation in an image, and cross-correlation between the images (Pardo-Iguzquiza et al., 2006). In this prediction, semi-variogram of target variable and covariable is estimated and the cross-variogram between them is estimated. They used sub-pixel information and modelling of covariance and cross-covariance. Pardo-Iguzquiza and Atkinson (2007) upgrade the method by using deconvolution method on estimated variogram and then deriving two downscaling weights which act as a high pass filter and low pass filter for the high resolution image and low resolution image. Further image fusion is applied to achieve downscaled image. The advantage of this technique is that it uses point support variogram model to downscale the image to the resolution of covariable. In this study the effect

of PSF on downscaling is considered. Pardo-Iguzquiza et al. (2006) consider point support function in deconvolution for downscaling algorithm.

2.7. Point spread function

Digital images are imperfect replica of the true objects. This imperfection is due to imaging system, signal noise, atmospheric effect mainly scattering, and shadows. A blurring effect in the digital images is due to aberration of lens, recording medium resolution, and atmospheric scatter. These effects together specified as point spread functions (Wolf and Dewitt, 2004) . Image of a point source is called point spread function (PSF). It describes the response of the sensor to radiance light from the given direction (Feng et al., 2004). PSF also describes pixel's non-uniform spatial information. Huang et al. (2002) studied the effect of sensor PSF on land product of MODIS in which the effect of uniform PSF and Gaussian PSF illustrated in figure 4 were studied.

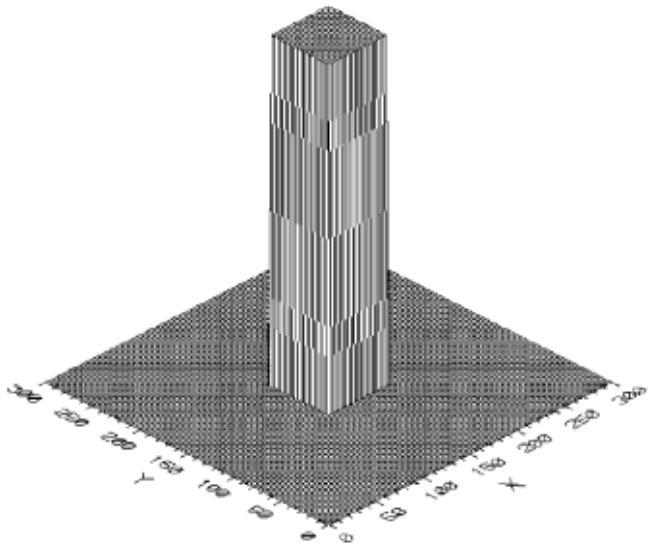

Figure 2-5 : Uniform PSF (Pardo-Iguzquiza and Atkinson, 2007)

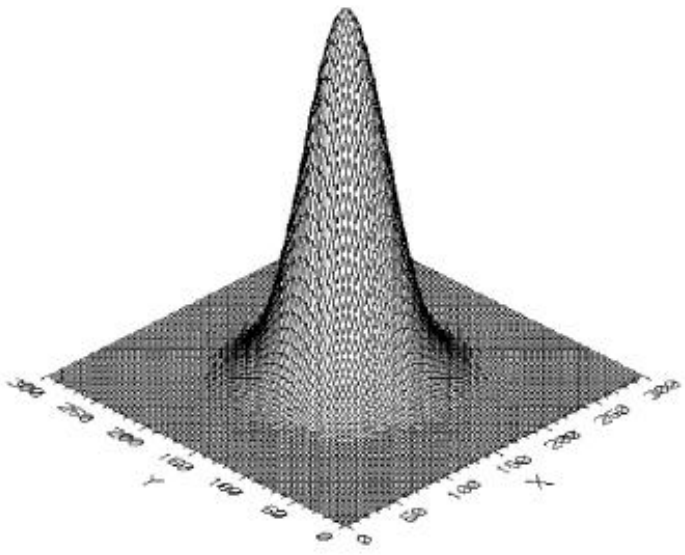

Figure 2-6 : Gaussian PSF (Pardo-Iguzquiza and Atkinson, 2007)

The quality of the image is more affected by the PSF, Gaussian PSF smoothen the image more than that of ideal PSF. The ideal PSF is the PSF which has uniform response from inside the pixel only and it is not affected by the response from outside of pixel while actual PSF is the PSF which has the effects from the surrounding. Actual PSF is the PSF of sensor. In this case Gaussian fit is more optimal and this Gaussian PSF is approximately same as actual PSF In this case Gaussian PSF is approximately same as actual PSF. Gaussian PSF changes pixel value while ideal PSF doesn't change the value from the original pixel value. PSF plays an important role during deconvolution it tunes the deconvolution process. It accurately estimates the pixel value from its surrounding. In this study uniform and Gaussian PSF are used for the deconvolution process. The role of deconvolution in this study is to built the relation between pixel support covariances and point support covariances (Pardo-Iguzquiza and Atkinson, 2007).

In this study an attempt is made to study the technicality of the downscaling cokriging algorithm and to estimate LAI at finer scale.

3. STUDY AREA AND DATA DESCRIPTION

To study the downscaling cokriging technique we require optical data of coarser spatial resolution and finer spatial resolution. We select barkot forest region for our study because forest plays an important role in global carbon cycle and ecological process.

3.1. Study Area

3.1.1. Selection of study area

Forest area near Dehradun district is selected as study area for this research. This area is surrounded by forests like Mohand forest, Barkot forest, Thano forest etc. The main focus of this study will be on Barkot forest is a tropical forest having sal species in major. Sal (*Shorea robusta*) is one of the important species of timber which is delicate and highly threatened from land use and development and also management practices (Singh, 2010).

3.1.2. Study area description

The study area is located in Dehradun, Uttarakhand, which is located between (30°31'55.20"to 29°54'27.54") N and (77°34'24.31" to 78°17'8.57") E at an average elevation of 647.09m. Dehradun is surrounded by dense forests, Rajaji national park and many species of vegetation. The study area has enormous and diverse vegetation in form of forests, agriculture land, road side plantations, etc. The study area is well connected to metalled roads which are connected to many link roads. These link roads are well connected to villages which make access to interior of the study site. The study site is connected to two rivers i.e. Song and Jakhan rivers. The average annual temperature of the area is 20° C and average annual rainfall of 2080mm. May and June are the hottest month and December and January are the coldest month of the year.

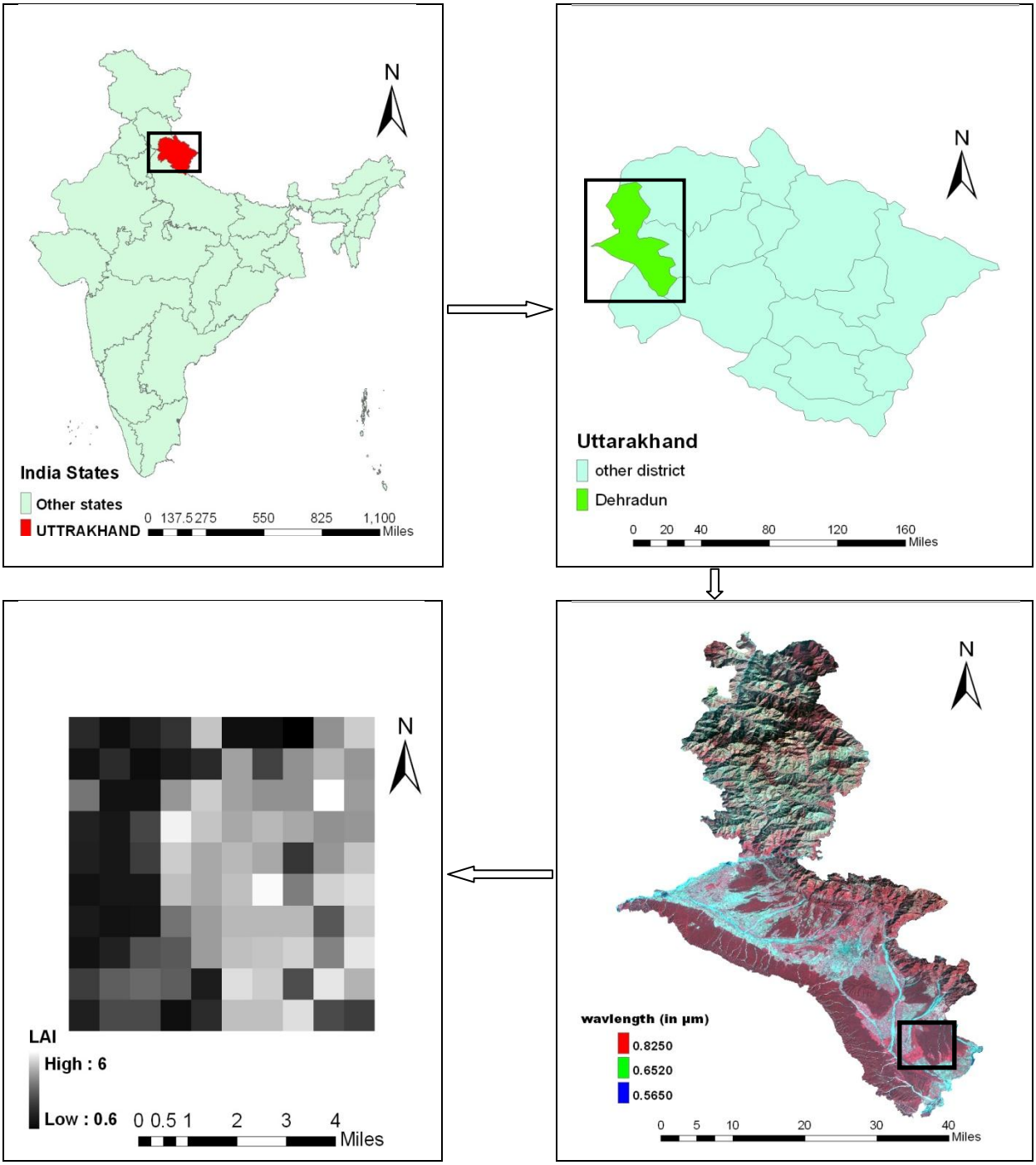

Figure 3-1 : Study area

3.2. Data used

3.2.1. Satellite data

Moderate-Resolution Imaging Spectroradiometer (MODIS) is a space-borne satellite sensor having 36 spectral bands of wavelength from 0.4 μm to 14.4 μm. It works in three spatial resolutions on 250 m, 500 m, and 1 km. There are 2 bands at 250 m, 5 bands at 500 m and 29 bands at 1 km. It is having a high temporal resolution (every 1 to 2 days). There are 3 platform Terra, Aqua and combined platform of Terra and Aqua. MODIS product is delivered in sinusoidal projection with 10° grid. It covers the whole globe in 36 tiles along east-west axis and 18 tiles along north-south axis of 1200 x 1200 km (Pandya et al., 2006a). MOD15A2 LAI/FPAR and MOD13Q1 product is used in this study which is a level 4 product. Level 4 products are final processed data which passes all the correction like geometric, radiometric, etc. Figure 3-2 shows the tiles covering the products, green color tile represent land product, blue tile represent ocean, pink tile represent sea-ice product and orange tile are land tile but product is not generated (Myneni et al., 2003)

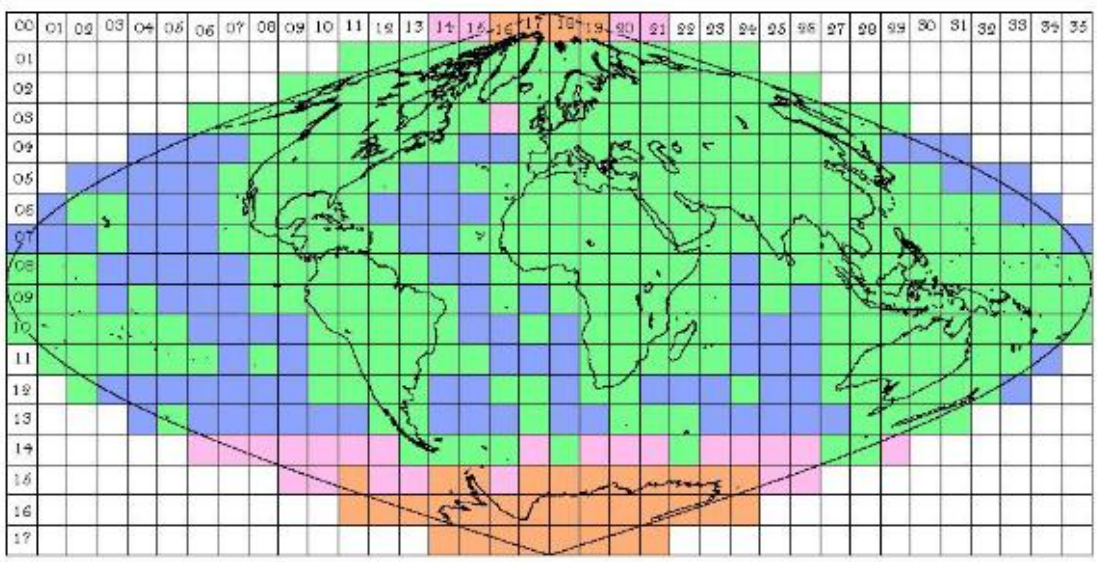

Figure 3-2 : The tiles covering MODIS product (Myneni et al., 2003)

- MOD15A2 (MODIS LAI) is 8 day terra product of 1 km. It is used as a primary variable for downscaling. Time of acquisition for this product is 11:00 AM IST and date is 16th October, 2011. MOD15A2 product is a 5 layer image i.e. LAI of 1 km pixel size, has 5 layers i.e. LAI product, FPAR product, FparLai_QC, FparExtra_QC, Std. deviation. The scale factor for LAI is 0.10 and for FPAR it is 0.01.

- MOD13Q1 is a 16 day NDVI product of 250 m from MODIS Terra sensor. This product is used as a covariable and participates in downscaling the primary variable by using downscaling cokriging. The product comprises NDVI, EVI, vegetation indices quality details, red reflectance band, NIR reflectance band, blue reflectance band, MIR

reflectance band, view zenith angle, sun zenith angle, relative azimuth angle, composite day of the year, and pixel reliability summary QA for 16 day at 250 m spatial resolution. It is in sinusoidal projection with 10° grid (DAAC, 2013).

4. MATERIALS AND METHODOLOGY

The main task of this study is to explore the downscaling cokriging technique using uniform and Gaussian point spread functions and to downscale LAI for the resources department. MODIS provide LAI product at 1000 m which is coarse spatial resolution and is not sufficient to study vegetation density at this scale (Hwang et al., 2011). So downscaling of the available coarse resolution product to fine resolution or desired resolution will resolve the above problem. For this study downscaling cokriging is used to downscale MODIS LAI product of 1000 m spatial resolution to 250 m spatial resolution. In this level it is downscaled to 250 m spatial resolution with the help of MODIS NDVI product of 250 m spatial resolution. It is necessary to calculate correlation between primary variable and covariable for cokriging.

4.1. Estimating correlation between LAI, NDVI, reflectance band (red, NIR)

To estimate correlation between primary variable and covariable is important in downscaling cokriging technique. In cokriging covariable must be correlated to the primary variable. MODIS LAI product, MODIS NDVI product and MODIS surface reflectance is used to estimate correlation. MODIS NDVI product is given at 250 m spatial resolution and MODIS surface reflectance is given at 500 m spatial resolution so both the products are aggregated to MODIS LAI 1000 m spatial resolution and then liner model of regression is applied to estimate correlation between them.

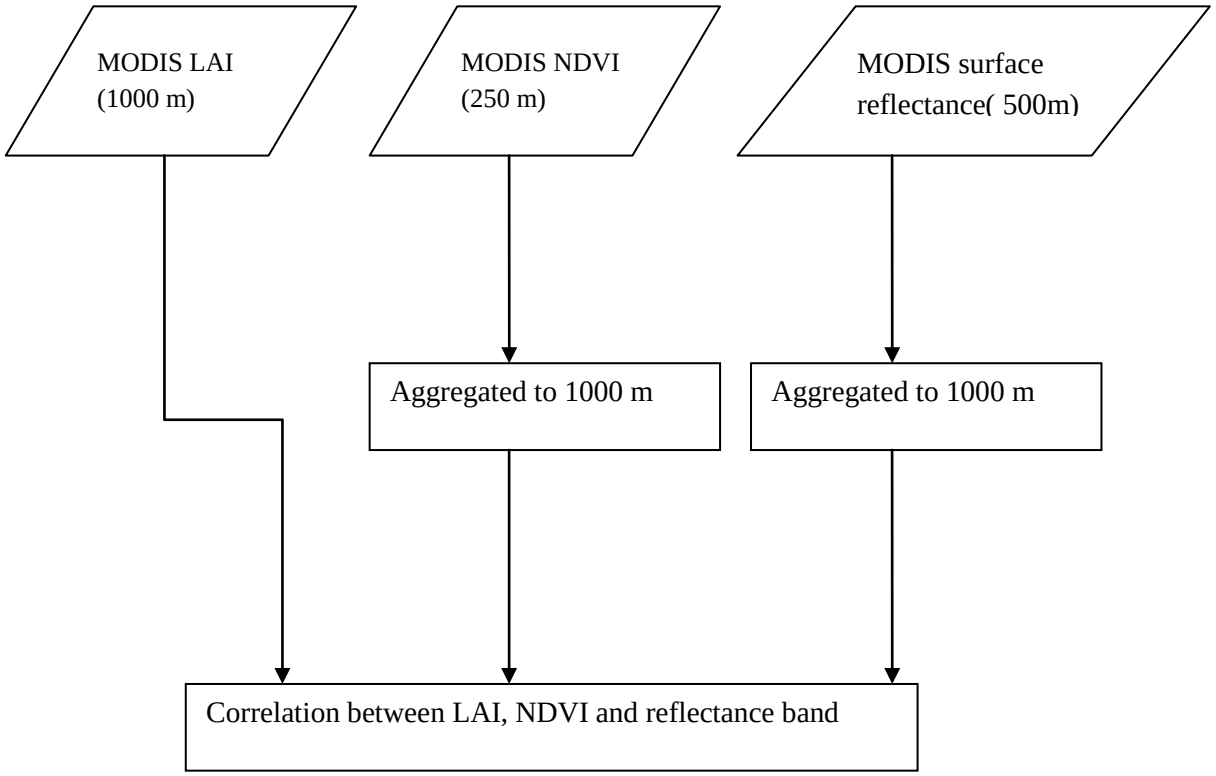

Figure 4-1 : Estimation of correlation between LAI and NDVI, red reflectance.

4.2. Resampling LAI from 1000 m to 250 m for calculating sample variogram

To calculate sample cross-variogram both variable at coarse and fine resolution should be on same scale, so to bring both the variable on common scale resampling has been conducted. In this, four type of resampling has been experimented i.e. nearest neighbour, bilinear interpolation, cubic convolution and trivial resampling. After resampling by these four techniques, cross-variogram has been calculated at constant cut-off of 6000 m, common bin of 15 and then best fit model is obtained at common range of 3817.4 m. To see the effect of resampling on variogram the difference in sill and nugget is observed. Then the results are compared and better resampling has been selected.

4.3. Modelling semi-variogram and cross-variogram for convolution and de-convolution using uniform PSF and Gaussian PSF.

Cokriging is unbiased predictor which minimizes the prediction variance. It considers the pixel support i.e. the pixel size of the image through semi-variogram and cross-variogram. This cokriging requires estimation of covariance and cross-covariance first. Pixel supports are modelled as the random function (RF) and further realization of these random functions is considered. All the realization images should be co-registered to avoid the mismatch of the pixel at different resolutions. MODIS NDVI 250 m is used as covariable for downscaling MODIS LAI 1000 m to 250 m spatial resolution. Pardo-Iguzquiza et al. (2006) explain the cokriging prediction by estimating the weights as:

$$\hat{Z}_u^k(x_0) = \sum_{i=1}^{N} \lambda_i^0 Z_u^l(x_i) + \sum_{j=1}^{M} \beta_j^0 Z_u^l(x_j) \qquad \text{Equation 4.1}$$

$\hat{Z}_u^k(x)$ Random variable of k spectral band estimated by cokriging for u (MODIS at 250 m) pixel size with spatial location $x_0\{x_1, x_2\}$.

$Z_V^k(x_i)$ Random variable of coarse spatial resolution with pixel size V (MODIS LAI at 1000 m) and spectral band k. The weight assigned to random variable of the i^{th} pixel is λ_i^0.

$Z_u^l(x_j)$ Random variable of k spectral band of fine spatial resolution image for u pixel size. The weight assigned to random variable of the j^{th} pixel is β_j^0.

N N of these pixels are used to predict spectral band k with support V in prediction of $Z_u^k(x)$

M M of these pixels are used to predict spectral band l with support u in prediction of $Z_u^k(x)$. Furthermore, variable are assumed o be second order stationary with constant mean.

λ_i^0 Weights assign to the random function $Z_V^k(x)$ at location (x_i) which is used to predict Z_u^k at location x_0

β_j^0 weights assign to the random function $Z_u^l(x)$ at location (x_j) which is used to predict Z_u^l at location x_0

Cokriging system can be expressed a matrix:

$$CL = B \qquad \text{Equation 4.2}$$

C is the matrix containing covariances or cross-covariances of experimental images
L is the matrix containing the unknown weights
B is the matrix which contains the cross-covariances which are not accessible experimentally (More information on these matrix is given by Pardo-Iguzquiza and Atkinson (2007).)

The unknown weights can be calculated as matrix C and B are calculated.

$$L = C^{-1} B \qquad \text{Equation 4.3}$$

Due to two problem in matrix B i.e. firstly the parabolic behaviour in covariances and cross-covariances which is caused by positive area of pixel support which doesn't capture this behaviour and secondly all covariances and cross-covariances must be positive definite it is not solved empirically (Pardo-Iguzquiza and Atkinson, 2007). So the above problem is solved by using theory of linear system and concept of random function with point support. Theory of linear system built a relation between point support covariance and pixel support covariance by using convolution of point covariance with the point spread function of the sensor (Pardo-Iguzquiza and Atkinson, 2007). In this study uniform PSF and Gaussian PSF is used. The uniform PSF has the constant all over the pixel which is given as:

$$h_v(y) = \begin{cases} \frac{1}{V}, & \text{if } y \in V \\ 0, & \text{otherwise} \end{cases} \qquad \text{Equation 4.4}$$

$h_v(y)$ represents the response of the pixel (v) at point support.
y represent a point support
V represents the support size

Gaussian PSF is given by Pardo-Iguzquiza et al. (2010) as:

$$h_v(s) = \begin{cases} \frac{1}{2\pi\sigma_x\sigma_y} \exp\{-\frac{1}{2}[\frac{x^2}{\sigma_x^2} + \frac{y^2}{\sigma_y^2}], & \text{if } s = \{x, y\} \in V' \\ 0, & \text{Otherwise} \end{cases} \qquad \text{Equation 4.5}$$

σ_x is the standard deviation along x axis
σ_y is the standard deviation along y axis
These σ_x and $\sigma_y$were chosen at 250 m for coarse spatial resolution and 122.5 m for fine spatial resolution after parameterizing these standard deviation. These standard deviations are parametrized by selecting many values for standard deviation and then estimating point support variogram were analyzed to check the variance. The standard deviation which gives the least variance is selected and further used to estimate PSF. Also these values were selected on basis of

scale factor on which primary and covariable is downscaled like LAI need to be downscaled at 250 m and standard deviation close to centre of the pixel of NDVI was selected.

Applying theory of linear systems to build the relation between covariance,

$$C_{VV}^{kk}(s) = C_{\bullet\bullet}^{kk}(s) * h_v(s) * h_v(-s)$$

Equation 4.6

$$= C_{\bullet\bullet}^{kk}(s) * \rho(s)$$

* is the convolution operator is used to multiply number of arrays of different or same sizes but of same dimensionality to produce another array of same dimensionality.

$\rho(s)$ is known as deterministic correlation and

$C_{\bullet\bullet}^{kk}(s)$ is the point support covariance of the image of the kth band

s is the vector between centre of the two pixel of area V

With the above method i.e. convolution, covariance and cross-covariance can be estimated with any support. Further, deconvolution method is used to obtain point covariance and point cross-covariance with the help of estimated point support covariance and cross covariance (Pardo-Iguzquiza and Atkinson, 2007). These theoretical semi-variogram and cross-variogram models are fitted to estimate covariances and cross-covariances models. These models are used in deconvolution process and also these nested models can be used to provide more information about the kind of model which should be used for point support covariances and cross-covariances.

Deconvolution process explained by (Pardo-Iguzquiza and Atkinson, 2007) is used to estimate point covariances and cross-covariances. These point covariances and cross-covariances are estimated by using experimental covariances and cross-covariace or model fitted to them. Since $C_{VV}^{kk}(s)$ is unknown so $C_{\bullet\bullet}^{kk}(s)$ is used to predict $\hat{C}_{VV}^{kk}(s)$ which is given Pardo-Iguzquiza and Atkinson (2007) as:

$$\hat{C}_{VV}^{kk}(s) = C_{\bullet\bullet}^{kk}(s) * h_v(s) * h_v(-s)$$

Equation 4.7

$$\check{C}_{VV}^{kk}(s) = \check{C}_{V\bullet\bullet}^{kk}(s) * h_v(s) * h_v(-s)$$

Equation 4.8

$\check{C}_{VV}^{kk}(s)$ is the modeled covariance

In similar model covariances and cross-covariance can be estimated which are more stable. Further optimization of de-convolution is carried out to obtain the optimized model for point covariances and cross-covariances. It is an iterative procedure to minimize some distance with the help of desired model. So this minimization procedure is iteratively used for each structure in order to obtain the set of covariances and cross-covariances which must be positive definite. These positive definite in term of positive point support covariance and cross-covariance are built by linear model of co-regionalization. Linear model of co-regionalization ensures that there should not be a negative variance and checks the matrix is positive definite. (More on linear model of co-regionalization is given by (Pardo-Iguzquiza and Atkinson, 2007).

4.4. Cokriging system to estimate the downscaling cokriging weights and to obtain the downscaled image.

To obtain the unbiased prediction the weight should be unbiased and also minimize the prediction variance, as given below:

$$E\{\hat{Z}_u^k(x_0)\} = E\{Z_u^k(x_0)\} = m^k \quad \text{Equation 4.9}$$

$E\{\hat{Z}_u^k(x_0)\}$ is the estimated variable which is assumed to be second order stationary with constant mean.

From equation 2 and 11

$$m^k = m^k \sum_{i=1}^{N} \lambda_i^0 + m^l \sum_{j=1}^{M} \beta_j^0 \quad \text{Equation 4.10}$$

For unbiased predictor $\sum_{i=1}^{N} \lambda_i^0 = 1$ and $\sum_{j=1}^{M} \beta_j^0 = 0$ which means the sum of the weights of variable Z_V^k should be equal to one and sum of the weights of the variable Z_u^l should be equal to zero. These weights behave like a low pass filter and high pass filter and these filters are applied to get desired fine spatial resolution image. This high pass filter is applied on the coarser image (MODIS LAI 1000 m) and low pass filter is applied to finer resolution image (MODIS NDVI 250 m) and then image fusion is applied to fuse both the images shown in figure 4-2.

In this fusion, 3 x 3 window is applied on the coarse resolution and 4 x 4 window is applied on the fine resolution image. The sixteen pixels from the centre of the pixel of coarse resolution are estimated and 4 x 4 window estimate pixel from the neighbourhood. Due to both coarse and fine resolution image comes at same resolution and then both the images are fused to obtain downscaled image at 250 m.

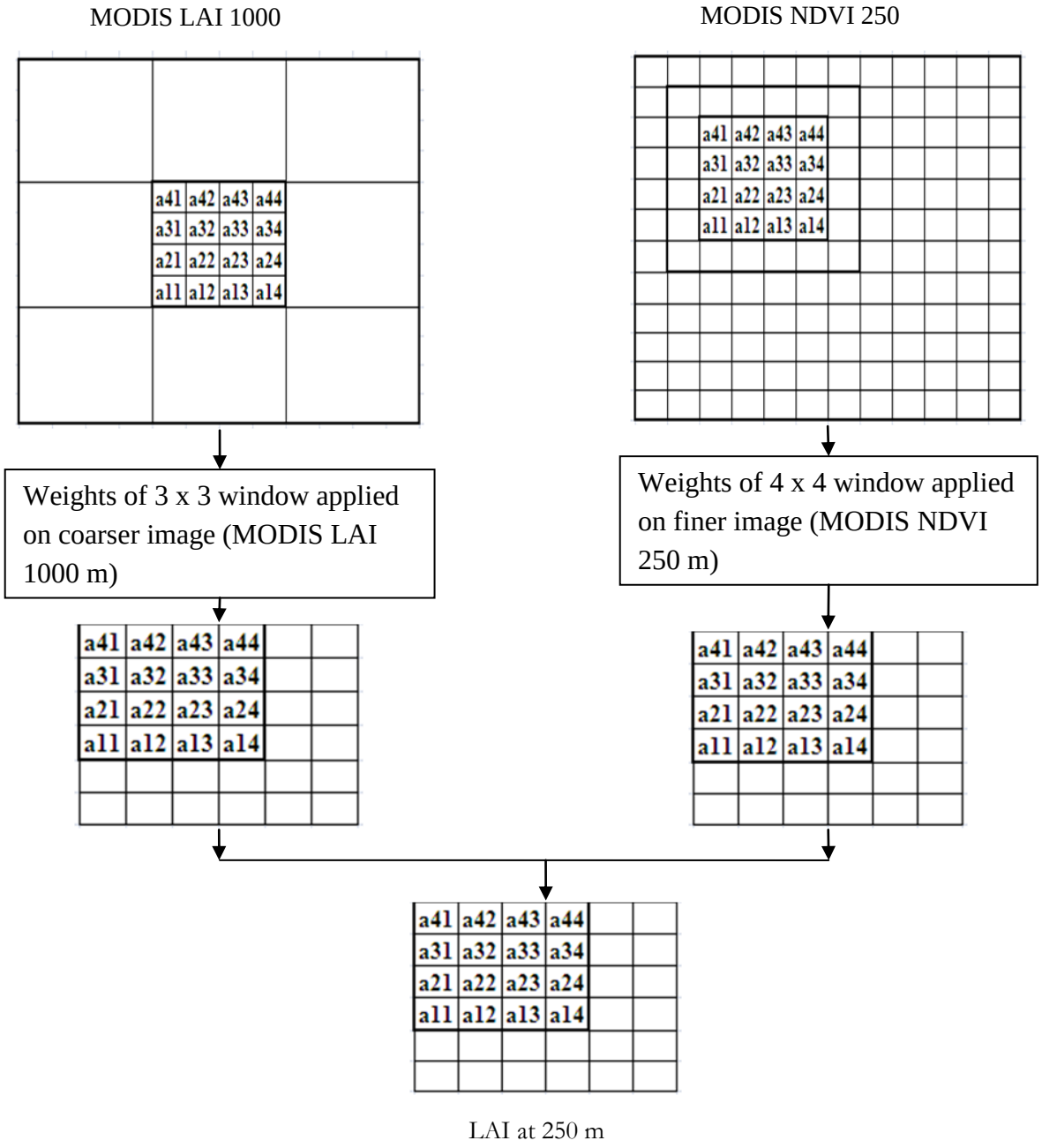

Figure 4-2 : Fusion of coarser and finer resolution image by applying cokriging weights to obtain downscaled MODIS LAI image at 250 m spatial resolution

4.5. Comparison of downscaled images obtained using uniform and Gaussian PSF

To analyze quality of downscaled MODIS LAI 1000 m image to 250 m spatial resolution descriptive statistics i.e. mean, median, standard deviation, minimum and maximum has been

calculated. Histogram and Box plot analysis were carried out to analyze the distribution of LAI value after downscaling by using uniform and Gaussian PSF. Auto-correlation of downscaled image has been calculated for spatial dependence and also use for comparison both the downscaled image.

4.6. Summary of the method

Methodology adopted in this research to achieve all the objectives is summarized below:-

- In this MODIS LAI 1000 m spatial resolution image is used to downscale to 250 m.
- MODIS data is given in sinusoidal projection. So, re-projection of MODIS data from sinusoidal to UTM projection is executed onto a WGS 84 datum by using MODIS conversion tool kit. The data are resampled by nearest neighbour techniques at the same time of re-projection.
- To select the covariable to downscale by using cokriging it is necessary to find the correlation between target variable and covariable. For this purpose correlation is estimated between MODIS LAI, MODIS NDVI, and MODIS surface reflectance. MODIS LAI has spatial resolution of 1000 m, MODIS NDVI has spatial resolution of 250 m and MODIS surface reflectance has spatial resolution of 500 m. So, all variable are aggregated to the common resolution to estimate correlation. Linear model of regression is applied to these variables in R software to estimate the p-value and R-squared value.
- The sample variogram of MODIS LAI 1000 m and MODIS NDVI 250 m were calculated. For the sample cross-variogram first MODIS LAI 1000 m has been resampled. To resample MODIS LAI at 250 m NN, CC, BI and trivial methods were used. Trivial resampling method pixels are degraded with equal value which is given in figure (4.3). Cross-variogram between LAI and NDVI at 250 m is calculated by using these techniques at common cut-off of 6000 m and bin of 15. Then these sample variogram were modelled using exponential model at common range of 3817.4. The effect of resampling was observed by comparing the sill and nugget and optimal resampling is selected by these comparisons.
  Here trivial resampling of MODIS LAI 1000 m to 250 m has been executed in which pixel are resample at 250 m in equal pixel value i.e. given in figure below:

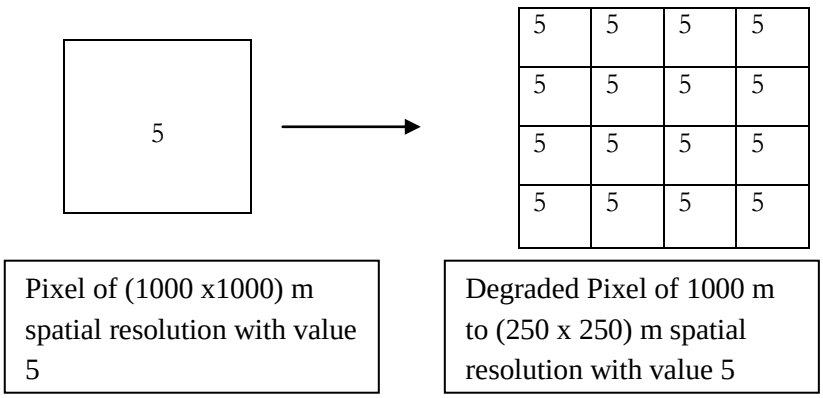

Figure 4-3 : Resampling by using trivial method.

- These variogram and cross-variogram were used to prepare parameter files for downscaling algorithm by Pardo-Iguzquiza et al. (2006) by using uniform (or the ideal PSF) and Gaussian PSF. For Gaussian PSF σ_x and $\sigma_y$are parameterized first and then optimal σ_x and σ_y are selected to estimate point support variogram and point support crosss-variogram.
- To study the impact of PSF on variogram estimated point support variogram and point support cross-variogram were analyzed.
- Then these regularized estimated point support variogram and cross-variogram are used to estimate cokriging weights using uniform and Gaussian PSF.
- Applying 3 x 3 weights (high pass filter) on the coarser image (MODIS LAI 1000 m) and 4 x 4 weights (low pass filter) are applied on finer resolution image (MODIS NDVI 250 m) for both uniform and Gaussian PSF.
- Then by image fusion finer resolution image MODIS LAI is obtained at 250 m for both the PSF.
- To study the impact of PSF on downscaling cokriging histogram and boxplot were estimated to show the difference in both the images and also descriptive statistics were compared for images obtained by both the PSF.

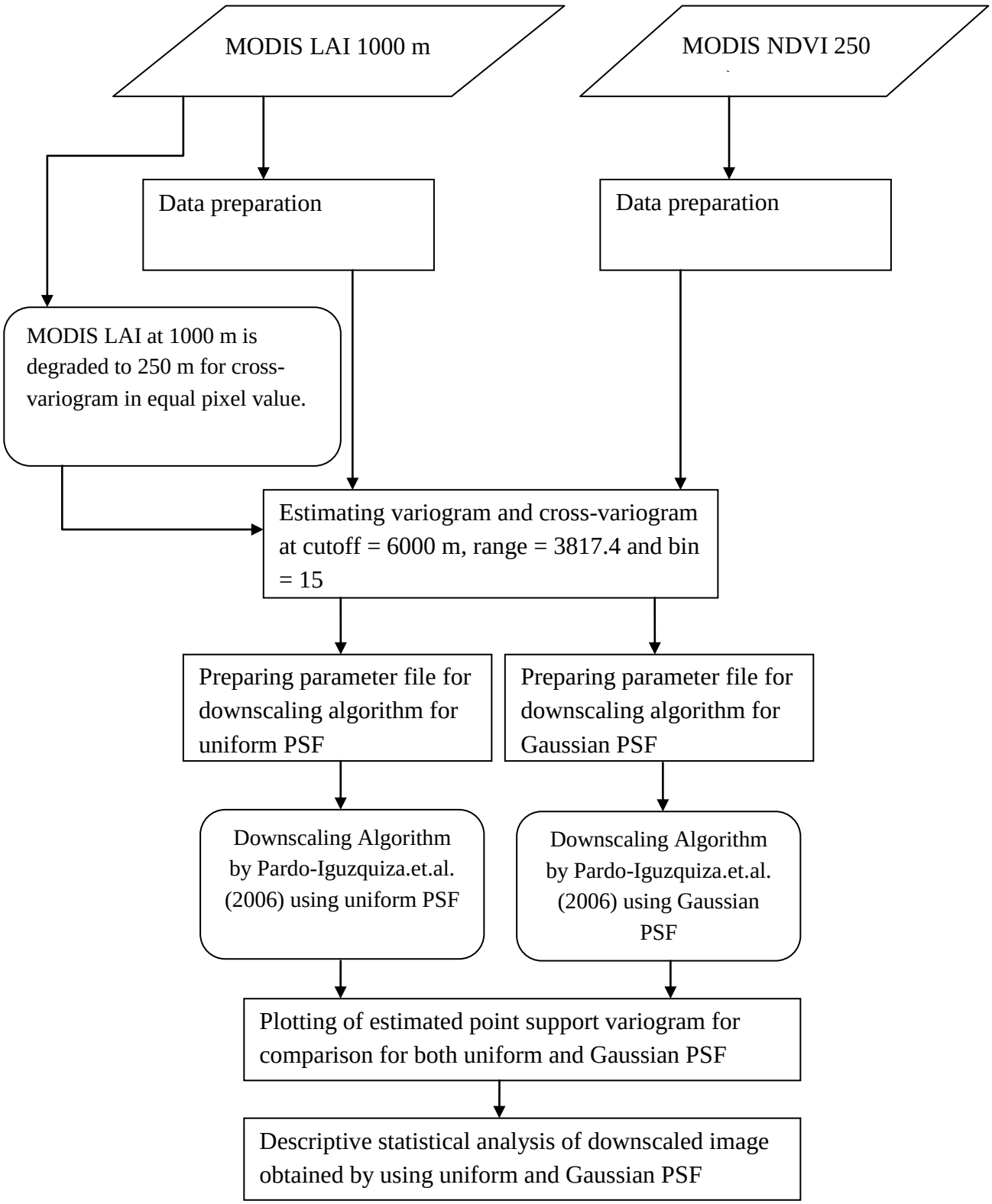

Figure 4-4 : Method adopted in this study

4.7. Software used

Table 4.1: Description of software used

S.No	Software	Used for
1	MODIS Conversion Tool-kit	Re-projection MODIS data from sinusoidal to UTM projection
2	Envi 5.0, ArcGIS 10	Creating subset of image, creating ASCII file, define projection of downscaled image
3	Force 2.0 (Fortran based compiler)	Downscaling cokriging algorithm
4	R Software	Estimating variogram, cross-variogram, descriptive statistics, estimating auto-covariances.
5	Notepad	To prepare parameter files for downscaling algorithm
4	Microsoft office 2007	Creating table , writing thesis

5. RESULTS

This chapter includes the main outcome of this study. In this chapter the downscaling algorithm is explored by using point spread function and also its effect of variogram and downscaling image. The results are divided under four major sections:

- Correlation of LAI with NDVI, NIR and Red bands
- Impact of resampling on the variogram and cross-variogram
- Impact of PSF on variogram
- Impact of PSF on downscaled image

5.1. Correlation of LAI with NDVI, NIR and Red bands from optical image

Correlation is used to find the relationship between two or more than two variables. In this study relationship is quantified by the correlation coefficient between LAI, NDVI, Near Infrared and red band which is shown in table 5.1.

Table 5.1 : Correlation of LAI with the variables NDVI, NIR and Red reflectance

Variable	p-value	R (correlation coefficient)
NDVI	<0.01	0.58
NIR	<0.01	0.47
Red	<=0.001	0.08

5.2. Impact of resampling on the variogram

In this study downscaling has been conducted from 1000 m spatial resolution to 250 m spatial resolution rather than 1000 m to 500 m because NDVI product is available at 250 m spatial resolution and at 500 m spatial resolution NDVI product is not availabe. To downscale LAI, cokriging is used because in cokriging covariable are used for prediction. In downscaling cokriging technique, cross-variogram is used to estimate cross covariances for convolution and deconvolution process, therefore for estimating the cross-variogram between MODIS LAI and NDVI must be on same resolution. So to bring coarser resolution at desired fine resolution MODIS LAI at 1000 m has been resampled. To see the effect of resampling sample cross-variogram were calculated by using four resampling techniques nearest neighbouring, bilinear interpolation, cubic convolution and trivial method on the variogram and cross variogram. To see the effect of resampling on variogram and cross-variogram each resampling has executed on LAI to resample and sample cross-variogram has been calculated which has been given below in the form of table and figure. Each sample variogram and cross-variograms are calculated by using common cut-off of 6000 and bin of 15 and then exponential model has been best fit at common range of 3817.4 m. For linear model of coregionalization the model is fixed to common range which is examine visually.

By using Nearest Neighbouring (NN) resampling on LAI, the nearest value is assigned to a pixel due to which there is not much change in the original value. The Figure (5-1) and table 5.2 shows the sill range and nugget of variogram of resampled LAI.

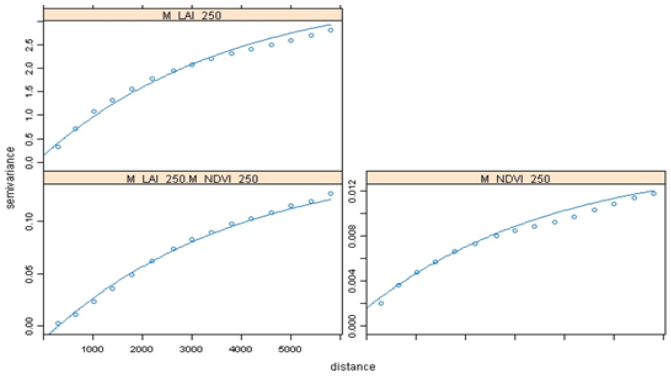

Figure 5-1 : Cross-variogram between MODIS NDVI 250 m and resampled LAI 250 m using NN resampling

Table 5.2 : Fitting of model to cross-variogram between MODIS NDVI 250 m and resample LAI 250 m for NN resampling

	Model	**Psill**	**Range**
M_LAI_250	**Exponential**	3.72	3817.44
M_NDVI_250	**Exponential**	0.01	3817.44
M_LAI_250.M_NDVI_250	**Exponential**	0.19	3817.44

By using Bilinear interpolation (BI) resampling, there is change observed in the value of sill and nugget which is shown in figure 5-2. It is also observed that the model is not properly fit at this constant range and shows more variance which is shown in figure (5-2) and table (5.3)

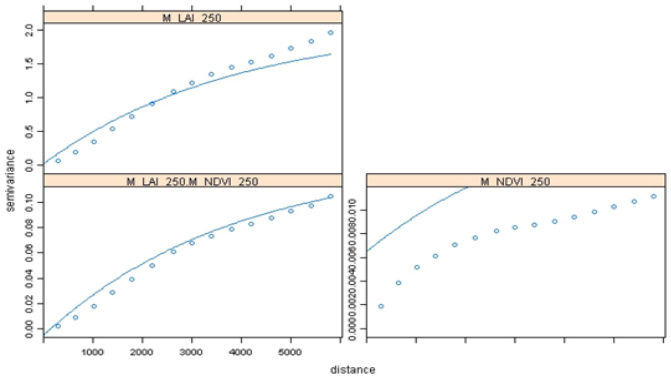

Figure 5-2 : Cross-variogram between MODIS NDVI 250 m and resample LAI 250 m using BI resampling

Table 5.3 : Fitting of model to cross-variogram between MODIS NDVI 250 m and resample LAI 250 m for BI resampling

	Model	Psill	range
M_LAI_250	**Exponential**	2.09	3817.44
M_NDVI_250	**Exponential**	0.013	3817.44
M_LAI_250.M_NDVI_250	**Exponential**	0.14	3817.44

By using Cubic convolution (CC) resampling, there is change observed in the sill and nugget. It is also observed that the model is not properly fit at this constant range and shows less variance which is shown in figure (5-3) and table (5.4)

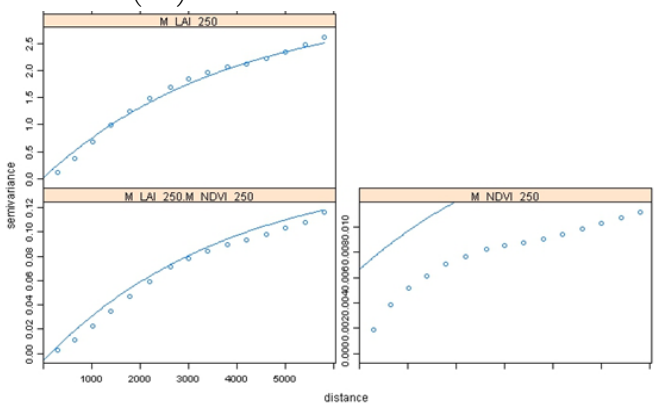

Figure 5-3 : Cross-variogram between MODIS NDVI 250 m and resample LAI 250 m using CC resampling

Table 5.4 : Fitting of model to cross-variogram between MODIS NDVI 250 m and resample LAI 250 m for CC resampling

	Model	Psill	range
M_LAI_250	**Exponential**	3.20	3817.44
M_NDVI_250	**Exponential**	0.01	3817.44
M_LAI_250.M_NDVI_250	**Exponential**	0.15	3817.44

By using trivial resampling, pixel is resampled at 250 m into equal original pixel values. The effect of trivial resampling is given in table (5.5)

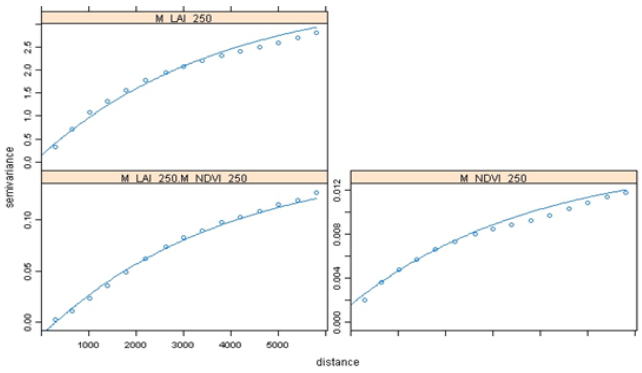

Figure 5-4 : Cross-variogram between MODIS NDVI 250 m and resample LAI 250 m using trivial resampling

Table 5.5 : Fitting of model to cross-variogram between MODIS NDVI 250 m and resample LAI 250 m for trivial resampling.

	Model	Psill	range
M_LAI_250	**Exponential**	3.78	3817.44
M_NDVI_250	**Exponential**	0.013	3817.44
M_LAI_250.M_NDVI_250	**Exponential**	0.21	3817.44

These tables 5-2 5-3 5-4 and 5-5 shows the change in sill and nugget at common range. Resampling by trivial method shows the highest variance among all four resampling applied. There is very close difference in the sill and nugget observe in the trivial method and NN resampling. Since there is no change in the pixel value trivial method is used as resampling for calculating sample cross-variogram and these sample variogram and cross-variogram point support covariance and cross-covariance is estimated by deconvolution in cokriging system.

5.3. Impact of PSF on variogram

Here for this study uniform PSF and Gaussian PSF are executed with downscaling cokriging. To study the impact of Gaussian PSF, σ_x (sigma x) and σ_y(sigma y) in equation 4.5 were first to set in order to estabilish the width and shape of the PSF. The width and shape of the PSF is responsible to characterize the imaging response to point signals. For this research, $\sigma_x$and σ_y are kept equal for coarse resolution (LAI) at 250 m and 122.5 m for fine resolution (NDVI). To parameterize σ_x and σ_y many values were used which shows its effect on spatial variability. There is more variance is observed in 250 m and 122.5 m sigma values. Further, these PSF has an effect on deconvolution which can be studied by point support variogram and cross-variogram. To model estimated point support variogram and cross-variogram nested exponential model was estimated. The estimated point support variogram from the downscaling cokriging for both the downscaled images of MODIS LAI 1000 m with uniform and Gaussian PSF were different for

empirical variogram of LAI and NDVI and same for cross-variogram. The point support variogram and cross-variogram are given below in figure 5-5 (a) and (b), 5-6 (a) and (b), 5-7 (a) and (b)

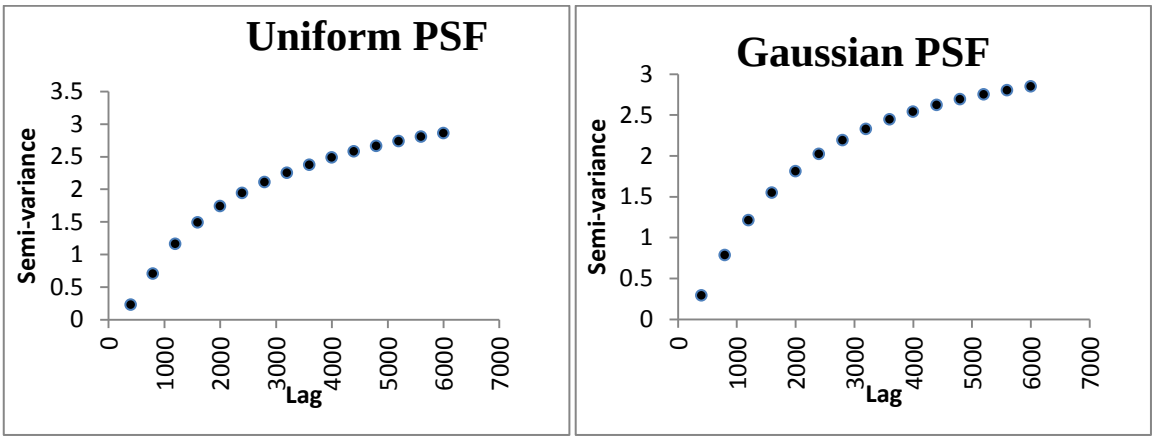

(a) (b)

Figure 5-5 : (a) Estimated point support variogram for MODIS LAI from 1000 m for uniform PSF (b) Estimated point support variogram for MODIS LAI from 1000 m for Gaussian PSF

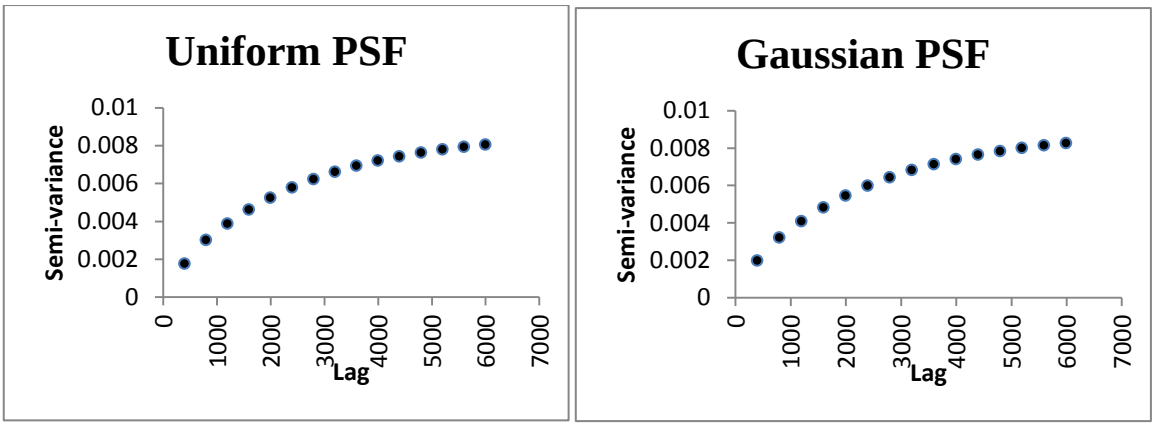

(a) (b)

Figure 5-6 : (a) Estimated point support variogram for MODIS NDVI from 250 m for uniform PSF (b) Estimated point support variogram for MODIS NDVI from 250 m for Gaussian PSF

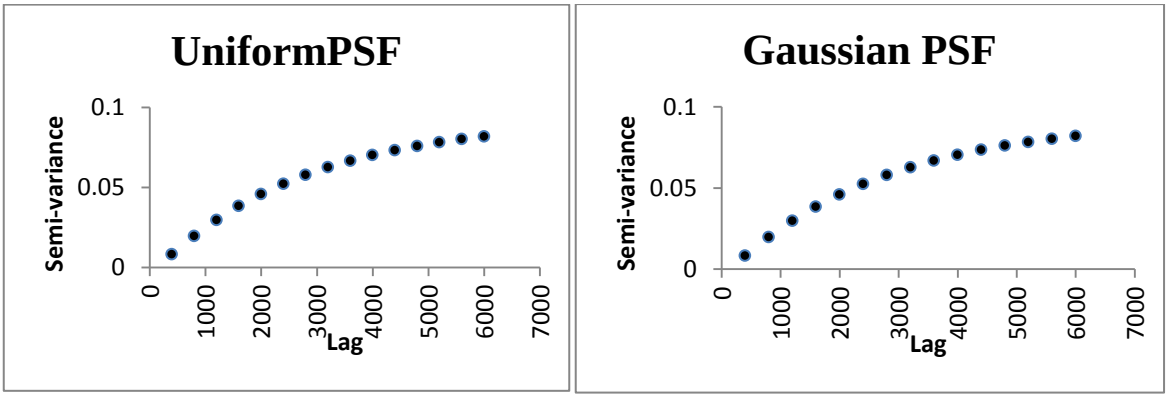

(a) (b)

Figure 5-7 : (a) Estimated point support cross-variogram between MODIS NDVI 250 m and resample LAI from 250 m for uniform PSF(b) Estimated point support cross-variogram between MODIS NDVI 250 m and resampled LAI from 250 m for uniform PSF

Table 5.6 : Modelled point support variogram for estimated point support variogram for MODIS LAI 1000 m

	MODIS LAI 1000 m			
	Uniform PSF		**Gaussian PSF**	
	First structure	**Second structure**	**First structure**	**Second structure**
Sill	1.75	2.85	1.75	2.06
Range (X)	481.52	3040.57	715.96	3857.09

Table 5.7 : Modelled point support variogram for estimated point support variogram for MODIS NDVI 250 m

	MODIS NDVI 250 m			
	Uniform PSF		**Gaussian PSF**	
	First structure	**Second structure**	**First structure**	**Second structure**
Sill	0.002	0.002	0.002	0.008
Range (X)	842.1	997.9	842.1	997.9

Table 5.8 : Modelled point support cross-variogram for estimated point support cross-variogram between MODIS NDVI 250 m and LAI resample at 250 m

	Cross variogram of MODIS LAI NDVI 250 m			
	Uniform PSF		**Gaussian PSF**	
	First structure	**Second structure**	**First structure**	**Second structure**
Sill	0.0015	0.097	0.0015	0.097
Range (X)	601.4	1201.5	601.4	1201.5

To see the effect of PSF on the variogram and cross variogram PSF is executed during downscaling cokriging. These downscaled images are analyzed by estimated point support variogram from the downscaled cokriging. After applying uniform and Gaussian PSF on MODIS LAI 1000 m it was found that there is change in estimated short range (Range (X)) for both the

PSF which is described in table 5-6. It is observed that range for the Gaussian PSF is more than the uniform PSF and also sill for Gaussian PSF is more than that of uniform PSF.

Using uniform and Gaussian PSF for NDVI does not show any change in sill and range as shown in table 5-7 but there is difference in the variogram where variance and lag was different which is shown in figure 5-6 (a) and 5-6 (b) and also minimum variance is very slightly less for uniform PSF i.e (0.000181) than Gaussian PSF i.e. (0.000154) which is negligible.

There is also no change seen in the sill and range of the estimated cross-variogram after using uniform and Gaussian PSF. As shown in table 5-8 it has been noticed that the sill and the range for both are similar for the first structure of uniform and Gaussian PSF and the sill and the range for second structure are also similar. There is also approximately no change in variogram as shown in figure 5-8 (a) and (b).

5.4. Impact of PSF on downscaling cokriging

There is impact of PSF on estimating the cokriging weights. The point support models are used for calculating these weights for both finer (MODIS LAI 1000 m) and coarser resolution images (MODIS NDVI 250 m). These weights act as a high pass filter and low pass filter. Once these weights are calculated then they are applied as a window to obtain desired fine resolution image. These weights are estimated with the use of support on the predicted variable given in equation 4.2.

It can be seen that there is change in the weights after applying the uniform and Gaussian PSF. The example of weight for 3 x 3 window applied on MODIS LAI 1000 m using uniform PSF is given in table 5-9 (a) and weight for 4 x 4 window applied on MODIS NDVI 250 m using uniform PSF is given in table 5-9 (b). Same using Gaussian PSF the example of weights for 3 x 3 window applied on MODIS LAI 1000 m and weights for 4 x 4 window applied on MODIS NDVI 250 m is given in table 5-10 (a) and 5-10 (b). The sum of the weights of the high pass filter applied on MODIS LAI 1000 m estimated image are nearly 1.0 and sum of the weights of low pass filter applied on MODIS NDVI 250 m estimated image are nearly zero which implies the unbiased condition to set up a unbiased cokriging system.

Table 5.9 :(a) Example of Cokriging weights of 3 x 3 window which act as high pass filter for coarser resolution image (MODIS LAI 1000 m) obtained by using uniform PSF (b) Example of Cokriging weights of 4 x 4 window which act as low pass filter for finer resolution image (MODIS NDVI 250 m) obtained by using uniform PSF

A11		
0.083	0.357	-0.146
0.198	0.668	-0.033
0.030	-0.182	0.027

A12		
0.042	0.407	-0.137
-0.098	0.924	-0.031
0.063	-0.186	0.017

A13		
0.003	0.380	-0.054
-0.180	0.916	0.043
0.030	-0.132	-0.008

A14		
-0.001	0.217	0.123
-0.162	0.734	0.222
0.002	-0.070	-0.065

(a)

a11			
-1.039	-0.667	-0.820	-0.751
0.835	0.373	-1.760	0.319
-0.396	1.352	5.855	2.518
0.159	-0.595	-2.845	-2.537

a12			
-1.103	-0.738	-0.821	-0.637
0.933	0.451	-1.688	0.332
-0.191	1.211	5.837	2.541
0.411	-0.731	-3.057	-2.747

a13			
-1.145	-0.707	-0.767	-0.478
1.058	0.410	-1.789	0.281
-0.358	1.261	5.947	2.458
0.073	-0.854	-3.206	-2.184

a14			
-0.935	-0.610	-0.692	-0.578
0.977	0.368	-1.830	0.176
-0.516	1.347	5.955	2.433
-0.206	-0.830	-3.066	-1.991

(b)

Table 5.10 : (a) Example of Cokriging weights of 3 x 3 window which act as high pass filter for coarser resolution image (MODIS LAI 1000 m) obtained by using Gaussian PSF: (b) Example of Cokriging weights of 4 x 4 window which act as low pass filter for finer resolution image (MODIS NDVI 250 m) obtained by using Gaussian PSF

B11		
0.285	0.228	-0.111
0.013	0.583	0.016
0.063	-0.047	-0.032

B12		
0.130	0.317	-0.122
-0.149	0.830	0.049
0.087	-0.108	0.034

B13		
0.035	0.396	-0.079
-0.169	0.722	0.144
0.047	-0.070	-0.027

B14		
-0.003	0.412	0.028
-0.095	0.349	0.321
- 0.012	0.034	-0.035

(a)

b11			
-2.476	-0.791	-0.746	-1.092
1.500	0.540	-2.551	0.721
-0.226	1.186	7.426	3.451
0.558	-0.321	-3.472	-3.706

b12			
-1.394	-0.847	-1.063	-0.891
1.026	0.831	-2.287	0.723
-0.174	1.156	8.099	3.313
0.927	-0.831	-4.724	-3.863

b13			
-1.368	-1.409	-1.124	-0.358
1.118	0.114	-2.510	0.409
-0.085	1.651	8.342	2.498
0.268	-1.539	-4.792	-2.214

b14			
-2.424	-1.347	-0.747	-0.463
1.602	0.843	-2.794	0.396
-0.020	1.582	7.669	2.659
-0.121	-0.906	-3.553	-2.374

(b)

These changes in weights may also show the effect of uniform and Gaussian PSF on downscaling cokriging because these weights are used to set up the ordinary cokriging system. These weights are also responsible for the prediction minimum variance and unbiased condition.

To study the effect of PSF on downscaling cokriging image descriptive statistics have been calculated i.e. histogram, box plot, minimum, maximum, 1st quartile, 2nd quartile, mean, median and standard deviation which is given in Table 5-11. This table explains changes at downscaling levels at uniform PSF and Gaussian PSF. The impact of PSF can be noticed on downscaled image in figure 5-8 and 5-9.

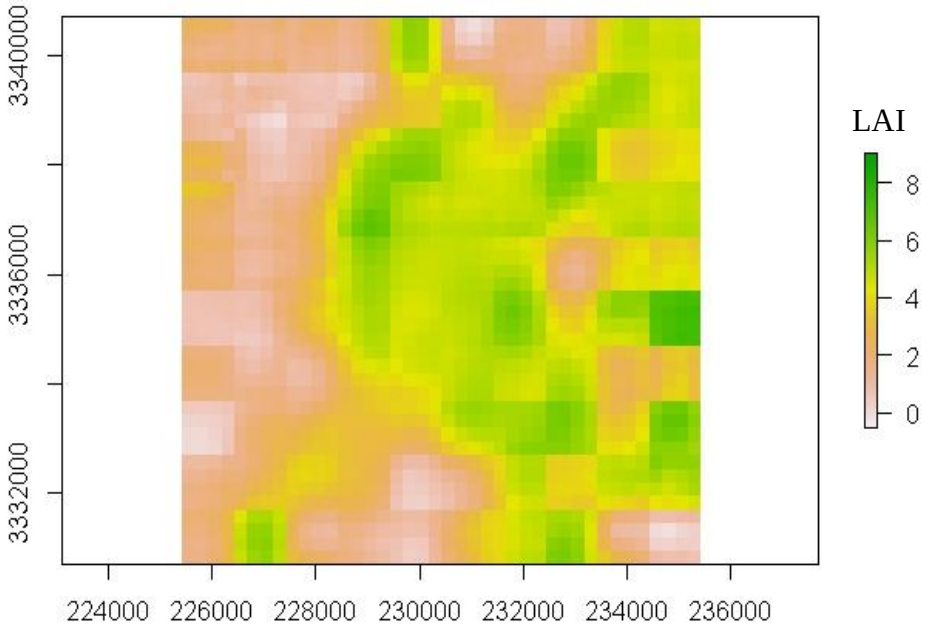

Figure 5-8 : Downscaled image of MODIS LAI at 250 m using uniform PSF

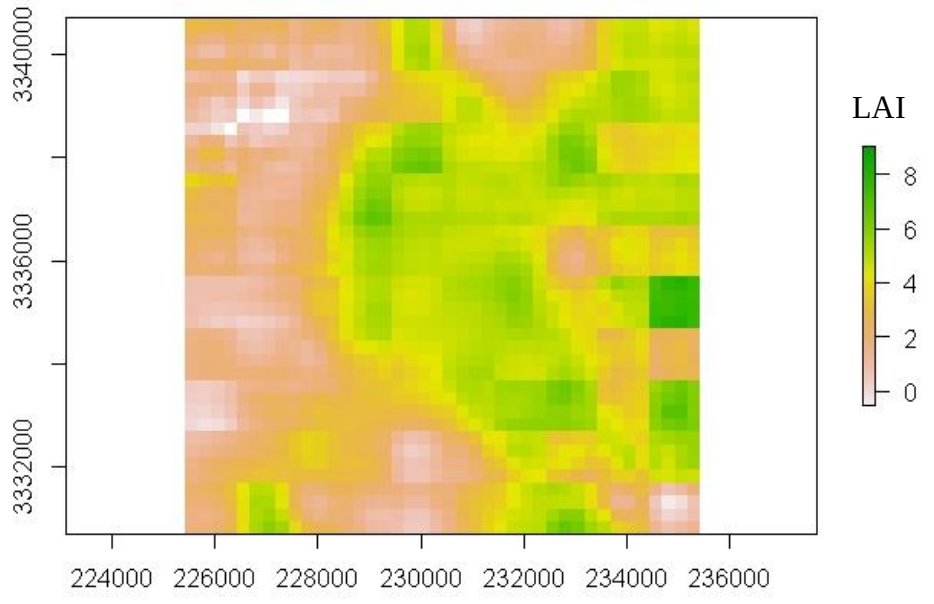

Figure 5-9 : Downscaled image of MODIS LAI at 250 m using Gaussian PSF

.

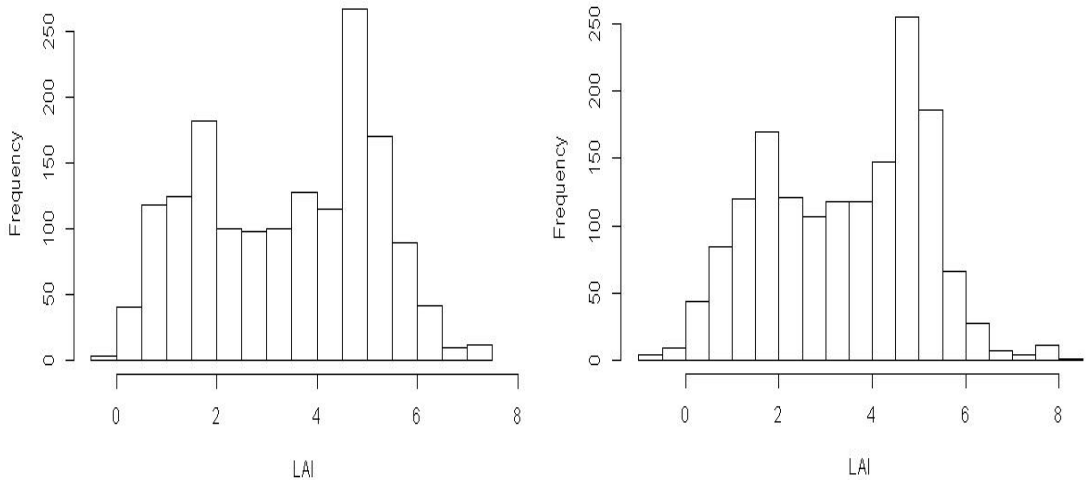

Figure 5-10 : (a) Histogram of LAI showing occurrence of downscaled MODIS LAI at 250 m using uniform PSF (b) Histogram of LAI showing occurrence of downscaled MODIS LAI at 250 m using Gaussian PSF

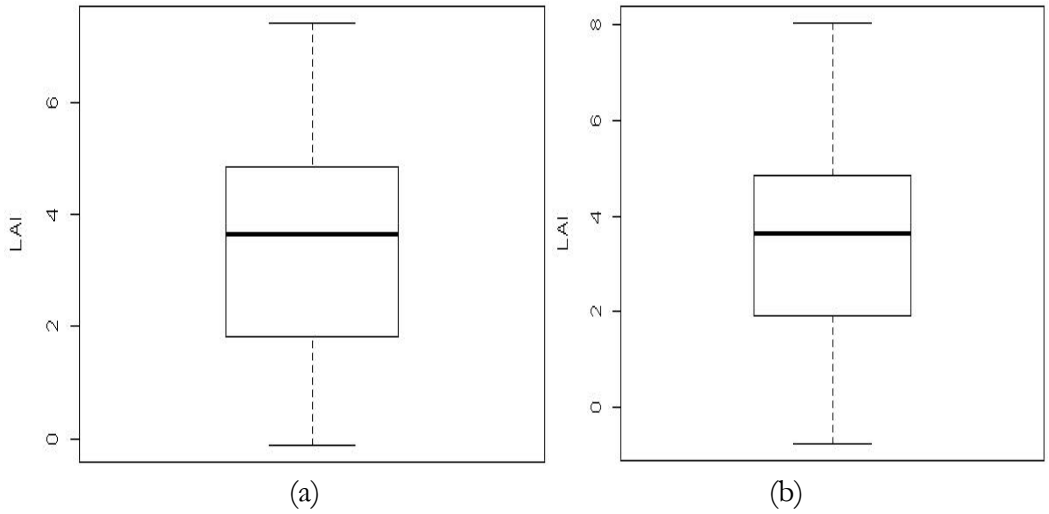

Figure 5-11 : (a) Boxplot of LAI showing distribution of downscaled MODIS LAI at 250 m using uniform PSF(b) Boxplot of LAI showing distribution of downscaled MODIS LAI at 250 m using Gaussian PSF

Histogram in figure 5-10 (a) and 5-10 (b) is showing the distribution of LAI at different downscaling level and it also shows LAI value from 4.5 to 5 has high occurrence in downscaled 250 m using uniform PSF and in figure 5-10 (b) the downscaled image with Gaussian PSF of 250 m has high occurrence in LAI value 4 to 5. From the histogram it can also be noticed that the range of LAI value are more in gaussian PSF than that of uniform PSF.

5.4.1. Comparison between downscaled image using uniform PSF and Gaussian PSF

Descriptive statistic has been calculated at different downscaling level which is given below in Table 5-11:

Table 5.11 : Spatial distribution of downscaled LAI value obtained by using uniform and Gaussian PSF

	With uniform PSF		With Gaussian PSF	
Disaggregation level		**4 x 4**		**4 x 4**
Pixel size (m)	1000	250	1000	250
Minimum	0.6	-0.108	0.6	-0.755
1st Quartile	1.775	1.808	1.775	1.911
Mean	3.405	3.407	3.405	3.408
Median	3.950	3.636	3.950	3.621
3rd Quartile	4.90	4.854	4.90	4.855
Maximum	6.0	7.408	6.0	8.032
SD	1.64	1.73	1.64	1.691

Descriptive statistics shows changes in the minimum, maximum, 1st quartile, 3rd quartile and standard deviation for downscaled image obtained using uniform and Gaussian PSF which can be observed in the box plot in figure 5.17 (a) and 5.17 (b). This has also been observed that there is approximately no change in mean and median and also there is increase in standard deviation while the resolution is increased using uniform and Gaussian PSF. To show the spatial dependence in downscaled image using uniform and Gaussian PSF auto-covariance is estimated for the 10th row in the image for maximum lag 10 which is given in table 5.11. Auto-covariance is the mesure of spatial dependece between different lags. This autocovariance is calculated by calculating covariance at sucessive lags. This auto-covariance shows the spatial association and spatial correlation between the variable. This auto-covariance depicts spatial variation and spatial dependence in the image. It is observed that as the lag is increasing correlation and auto-covariance is decreasing. It is found that using uniform PSF there are some negative value at lag 9 and 10.

Table 5.12: Auto-covariance between downscaled image using uniform and Gaussian PSF

	Using Uniform PSF		Using Gaussian PSF	
Lag	Cov	r(correlation)	Cov	r(correlation)
0	2.95	1	2.89	1
1	2.86	0.96	2.74	0.94
2	2.56	0.86	2.52	0.87
3	2.11	0.71	2.24	0.77
4	1.60	0.54	1.86	0.64
5	1.13	0.38	1.56	0.54
6	0.70	0.23	1.22	0.42
7	0.34	0.11	0.87	0.30
8	0.07	0.02	0.57	0.19
9	-0.08	-0.02	0.36	0.12
10	-0.15	-0.05	0.20	0.07

5.5. Summary of the Results

The results obtained from this research are summarized on the effect of resampling on variogram, effect of PSF on variogram and downscaling cokriging.

It was found that trivial method is better to resample coarse resolution (LAI) to calculate sample cross-variogram. This technique shows more variance than the other resampling techniques. The uniform PSF shows the more spatial dependence than the Gaussian PSF.

Due to spatial variability or change in variance in point support variogram and cross-variogram the cokriging weights were found different for both the PSF and further which show changes in the downscaled cokriging image. These changes in the spatial distribution are explained by calculating minimum, maximum, mean, standard deviation in the LAI values. To show the spatial dependence auto-covariance was estimated which shows that uniform PSF has more spatial dependence than the Gaussian PSF.

6. DISCUSSION

The research has demonstrated the effect of resampling and PSF on downscaling cokriging technique by showing the selection of covariable by estimating the coefficient of correlation, the effect of resampling on variogram and cross-variogram, effect of PSF on variogram and cross variogram and effect of PSF on downscaling cokriging.

6.1. Correlation of LAI with NDVI, NIR and Red bands from optical image

Cokriging is multivariate area-to-point prediction approach. Downscaling using cokriging require a covariable to downscale LAI (primary variable). This covariable must have a relationship with primary variable. In this study for selecting the covariable correlation analysis has been done. Correlation analysis has been executed between primary variable LAI and covariable NDVI, Near Infrared reflectance band and red reflectance bands which are shown in table 5.1. From correlation analysis the relationship between LAI and NDVI is found positive ($r = 0.58$) and significant ($p < 0.01$). (Kale et al., 2005) found in his study that for relationship between LAI and NDVI the minimum correlation is $r = 4$ and maximum correlation is $r = 7.4$. In the month of October Barkot forest is full of vegetation due to which NDVI is high. Due to this high NDVI the correlation with LAI is high. Correlation of NIR ($r = 0.47$) is found less than NDVI with LAI at significant ($p < 0.01$) which is less than correlation with NDVI. A small relationship was found between LAI and red reflectance ($r = 0.001$) at significant ($p < = 0.001$). (Kaufman et al., 2002) stated that low correlation for the red reflectance is due to mixed vegetation and bright soil and red reflectance show high absorption in vegetation due to chlorophyll absorption. So relationship between LAI and NDVI is found more in compare to NIR and red reflectance.

6.2. Impact of resampling on the variogram and cross variogram

In this study coarser resolution image (MODIS LAI 1000 m) and finer resolution image (MODIS NDVI 250 m) is combinined to predict finer resolution image of MODIS LAI at 250 m. To estimate cross-variogram for estimating cross-covariance coarser and finer resolution were brought to a common resolution by resampling technique. NN, CC, BI and trivial resampling methods were executed to resample pixel of coarser resolution to finer resolution. The sample cross-variogram were calculated to see the effect of resampling at the common cut-off of 6000 m, bin of 15 and then modelled by using exponential model at a common range of 3817.4 m. This common range was choosen visually for linear model of coregionalization.

It was observed from the table 5-2, 5-3, 5-4, 5-5 that the sill and nugget are varying for all resampling methods in sample cross-variogram. It was observed that model was best fit to NN resampling and trivial resampling. The sill from trivial and NN resampling was found to be higher than that of CC and BI resampling which depicts that the variance is high at the range of 3817.4 in NN and trivial resampling. This high variance may be due to the resampled LAI value. In trivial method the values remain same, while in the nearest neighbour resampling the values

was approximately the same because it interpolates by taking the average of the nearest pixel value whereas the variance in CC and BI resampling is low due to which there is less spatial structure. So, for this research the trivial method was used in calculating sample variogram.

6.3. Impact of PSF on variogram and cross-variogram

The impact of the PSF on the variogram was studied by estimating the variogram to estimate point support variogram. These point support variogram were estimated for both the image using uniform and Gaussian PSF. In this study point support variogram were modelled by nested exponential structure of variogram at a common cut-off of 6000 m and bin of 15. It has been observed that for MODIS LAI 1000 m modelled point support variogram has a sill for first structure of 1.75 for uniform and Gaussian PSF at different range of 481.52m and 715.96 m and sill for second structure is 2.85 for uniform PSF and 2.068 for Gaussian PSF at range of 3040.57 m and 3857.09 m which is shown in table 5-6. It could be due to weight contributing in the pixel for Gaussian function which is more in the centre of pixel than the border of the pixel and for uniform PSF weights are uniform in the centre and at the border of the pixel. This change in sill may be due to the distance from the centre of the pixel is high. The distance from the centre of pixel is more for uniform PSF rather than Gaussian PSF which is shown in figure 5-5 (a) and (b). It can be noticed that for the same distance there is change in the variance which is due to change of pixel value which is high using uniform PSF.

Impact of PSF was not seen in the modelled point support variogram from MODIS NDVI 250 m as shown in table 5.7. The sill and the range of the first structure of uniform PSF and Gaussian PSF are same and for second structure sill and range are same, but there is a change in point supports variogram which can be observed in figure 5-6 (a) and (b). This change may be due to effect of σ_x and $\sigma_y$which affects the imaging response of the image where the response within the pixel is uniform and very less response from the outside of the pixel which may be due to atmospheric effect and geometry of the view (Huang et al., 2002)

Also no change has been noticed in the sill and the range of modelled estimated point support cross-variogram after using uniform and Gaussian PSF. As shown in table 5.8 it has been noticed that sill and range for the first structure of uniform PSF are similar and sill and the range for the second structure of uniform PSF and Gaussian PSF are similar and there is a no change in the point support cross-variogram also because there is no effect of PSF in point support cross-covariances (Pardo-Iguzquiza et al., 2006)

6.4. Impact of PSF on downscaling cokriging

To study the effect of PSF on downscaling cokriging the change in the weights are analyzed. As PSF plays an important role in setting up the unbiased cokriging weights for the ordinary cokriging system. Cokriging predictor is the function of cokriging weights and random variable. These random variables are related to variance which implies that variance is related to the cokriging weights. This indicates that if variance is high then weights will be high (Pardo-

Iguzquiza et al., 2011). The variance is high using uniform PSF rather than Gaussian PSF. From the table 5-9 and 5-10 it is observed that for uniform PSF and Gaussian PSF weights are different which is due to variance and for uniform PSF weights are more than that of Gaussian PSF. It can be also observed from the table 5-9 (a) and 5-10 (a) that the centre value of weights obtained by using uniform PSF is more than that of Gaussian PSF. Gaussian PSF is related to standard deviation in the pixel while uniform PSF does not involve the standard deviation. This indicates that the mean of the centre pixel of Gaussian support is more than that uniform PSF which affect the centre of the weights in inversely, as this mean is subtracted from the random function in the cokriging predictor so large is the mean small will be the weights.

It is also observed from the figure 5-8 and 5-9 that due to weights applied for downscaling, a blurring effect is visualized in downscaled image using gaussian PSF. It can be observed that the variance is less using Gaussian PSF than using uniform PSF due to which it is more difficult to visualize the object. This is due to the less spatial variability and smoothness in the image.

To study the effect of PSF on the downscaled images histogram has been estimated. Histogram in figure 5.10 (a) and 5.10 (b) it is observed that distribution of LAI value is approximately same for both the downscaled image using uniform and Gaussian PSF. In descriptive statistics from table 5-11 it is observed that there changes in minimum, maximum, 1st quartile, 3rd quartile and standard deviation in downscaled image using uniform and Gaussian PSF. This variation show there is a spatial variability in the downscaled LAI value though there is no clear pattern found. It is observed that standard deviation is more in uniform PSF which shows that there are more changes in LAI value than the Gaussian PSF though it depends on the distance from the centre of the pixel. It is also observed from table 5-12 that with the increase in the distance between the point pairs covariance decreases and also correlation also decreases. It is also observed that using Gaussian PSF covariance and correlation between the variables are higher and positive which shows the data at a closer distance are more similar to each other and using uniform PSF it is less spatially dependent because of gradual change in pixel in downscaled image using gaussian PSF.

7. CONCLUSION AND RECOMMENDATIONS

7.1. Conclusions

The main objective of this research is to study the effect of resampling and PSF on downscaling cokriging technique for LAI estimation. To achieve this objective four research questions were carried out in this study. An attempt is made to answer these research questions and conclusion for each question is given as:

1. What is the suitable covariable and its correlation with LAI?

NDVI and LAI relationship has been used to estimate LAI which has been seen in many researches as mentioned in literature review point 2.5. From this study it was found that out of variable considered i.e. infro-red, red and NDVI, NDVI is a suitable covariable to downscale LAI, though it shows a good relationship with LAI. Red reflectance and NIR reflectance does not show good relationship with LAI. It can be seen from the table 4.1 that correlation between LAI and NDVI is r = 5.8.

2. What is the effect of resampling on variogram and cross-variogram?

It was shown from the results 5.2 that there is change observed by applying the different resampling techniques. The NN and trivial method shows a high variance which means that there is more spatial structure. The trivial method is used for calculating the sample cross-variogram because of more spatial structure and the values did not changes after resampling of LAI from 1000 m to 250 m.

3. What is the effect of PSF on variogram and cross-variogram?

It was found from this study that for coarser resolution there is a change noticed in the estimated point support variogram using uniform PSF and Gaussian PSF. This change is due to the mean and standard deviation within the pixel. The change in the PSF is due to the response by distance from the centre of the pixel. The effects are also due to effect within the pixel and outside of the pixel while no change was observed in the cross-variogram.

4. What is the effect of PSF on resultant downscaled image?

To study the effect of PSF on downscaled image change in weight were observed at different PSF i.e. uniform and Gaussian PSF. Cokriging weights are related to covariance and cross-covariance. It was observed that variance is high in uniform PSF so the weights were high for the uniform PSF. These variances can be observed from the analysis of estimated point support variogram by observing sill, nugget and range. It is also found that quality of the image also depends on the PSF. Gaussian PSF shows the better quality than by using uniform PSF

Finally it is concluded that for NDVI is a suitable covariable to downscale LAI. Resampling by trivial method is optimal because it does not affect the LAI value after resampling. Point support function involved in the prediction has an effect on the estimating point support covariance and cross-covariance. The effect of PSF can be studied on estimating point support variogram and cross-variogram. The effect of PSF on the downscaled cokriging image can be observed by change in the cokriging weights. This change in the weights is due to variation in the covariance

and cross-covariance, centre mean of the pixel and the distance between point pairs. It is also observed that downscaled image using Gaussian PSF is more spatially dependent than using uniform PSF due to more variance in constant PSF.

7.2. Recommendation

The downscaling cokriging downscaling is performed on a target variable by using covariable. More than one covariable can be used to perform downscaling. Ground measurement and thematic maps may be considered as covariable. Different study area can be used. User define PSF may be used to study the PSF effect. This study may be carried out with different window size and study its effect. Different standard deviation may be experiment and field must be used for the validation.

REFERENCES

Asner, G.P., Braswell, B.H., Schimel, D.S., Wessman, C.A., 1998. Ecological research needs from multiangle remote sensing data. *Remote Sensing of Environment* 63(2), 155-165.

Asner, G.P., Scurlock, J.M.O., A. Hicke, J., 2003. Global synthesis of leaf area index observations: implications for ecological and remote sensing studies. *Global Ecology and Biogeography* 12(3), 191-205.

Atkinson, P.M., 2012. Downscaling in remote sensing. *International Journal of Applied Earth Observation and Geoinformation*.

Atkinson, P.M., Curran, P.J., 1995. Defining an optimal size of support for remote sensing investigations. *IEEE Transactions on Geoscience and Remote Sensing*, 33(3), 768-776.

Atkinson, P.M., Cutler, M.E.J., Lewis, H., 1997. Mapping sub-pixel proportional land cover with AVHRR imagery. *International Journal of Remote Sensing* 18(4), 917-935.

Baboo, S.S., Devi, M.R., 2010. An analysis of different resampling methods in Coimbatore, district. *Global Journal of Computer Science and Technology* 10(15), 61-66.

Bannari, A., Morin, D., Bonn, F., Huete, A.R., 1995. A review of vegetation indices. *Remote Sensing Reviews* 13(1-2), 95-120.

Baret, F., Guyot, G., 1991. Potentials and limits of vegetation indices for LAI and APAR assessment. *Remote Sensing of Environment* 35(2–3), 161-173.

Chen, J.M., Leblanc, S.G., 1997. A four-scale bidirectional reflectance model based on canopy architecture. *IEEE Transactions on Geoscience and Remote Sensing*, 35(5), 1316-1337.

Curran, P., 1980. Relative reflectance data from preprocessed multispectral photography. *International Journal of Remote Sensing* 1(1), 77-83.

DAAC, U.L., 2013. https://lpdaac.usgs.gov/products/modis_products_table/mod13q1. (accessed 7 January).

eXtension, 2008. Remote sensing resampling methods. http://www.extension.org/pages/9628/remote-sensing-resampling-methods (accessed February 1, 2013).

Fassnacht, K.S., Gower, S.T., MacKenzie, M.D., Nordheim, E.V., Lillesand, T.M., 1997. Estimating the leaf area index of North Central Wisconsin forests using the landsat thematic mapper. *Remote Sensing of Environment* 61(2), 229-245.

Fassnacht, K.S., Gower, S.T., Norman, J.M., McMurtric, R.E., 1994. A comparison of optical and direct methods for estimating foliage surface area index in forests. *Agricultural and Forest Meteorology* 71(12), 183-207.

Feng, C., Ma, J., Chen, J., 2004. The PSF correction method for satellite image restoration, IEEE First Symposium on Multi-Agent Security and Survivability, 2004 pp. 31-34.

Goldsmith, N., 2009. Resampling raster images. http://www.jiscdigitalmedia.ac.uk/stillimages/advice/resampling-raster-images/ (accessed February 1, 2013).

Goodale, C.L., Apps, M.J., Birdsey, R.A., Field, C.B., Heath, L.S., Houghton, R.A., Jenkins, J.C., Kohlmaier, G.H., Kurz, W., Liu, S., Nabuurs, G., Nilsson, S., Shvidenko, A.Z., 2002. Forest carbon sinks in the northern hemisphere. *Ecological Applications* 12(3), 891-899.

Gower, S.T., Kucharik, C.J., Norman, J.M., 1999. Direct and Indirect Estimation of Leaf Area Index, fAPAR, and Net Primary Production of Terrestrial Ecosystems. Remote Sensing of Environment 70(1), 29-51.

Hu, J., Tan, B., Shabanov, N., Crean, K.A., Martonchik, J.V., Diner, D.J., Knyazikhin, Y., Myneni, R.B., 2003. Performance of the MISR LAI and FPAR algorithm: a case study in Africa. Remote Sensing of Environment 88(3), 324-340.

Huang, C., Townshend, J.R.G., Liang, S., Kalluri, S.N.V., DeFries, R.S., 2002. Impact of sensor's point spread function on land cover characterization: assessment and deconvolution. *Remote Sensing of Environment* 80(2), 203-212.

Hwang, T., Song, C., Bolstad, P.V., Band, L.E., 2011. Downscaling real-time vegetation dynamics by fusing multi-temporal MODIS and Landsat NDVI in topographically complex terrain. Remote Sensing of Environment 115(10), 2499-2512.

Jeganathan, C., Hamm, N., Mukherjee, S., Atkinson, P.M., Raju, P.L.N., Dadhwal, V.K., 2011. Evaluating a thermal data sharpening technique over a mixed agricultural landscape in India. *International Journal of Applied Earth Observation and Geoinformation* 13, 178-191.

Jonckheere, I., Fleck, S., Nackaerts, K., Muys, B., Coppin, P., Weiss, M., Baret, F., 2004. Review of methods for in situ leaf area index determination: Part I. Theories, sensors and hemispherical photography. *Agricultural and Forest Meteorology* 121(1–2), 19-35.

Kale, M., Singh, S., Roy, P.S., 2005. Estimation of Leaf Area Index in dry deciduous forests from IRS WiFS in central India. *International Journal of Remote Sensing* 26(21), 4855-4867.
Kaufman, Y.J., Gobron, N., Pinty, B., Widlowski, J., Verstraete, M.M., 2002. Relationship between surface reflectance in the visible and mid-IR used in MODIS aerosol algorithm - theory. *Geophysical Research Letters* 29(23), 2116.

Kustas, W.P., Norman, J.M., Anderson, M.C., French, A.N., 2003. Estimating sub-pixel surface temperatures and energy fluxes from the vegetation indexradiometric temperature relationship. *Remote Sensing of Environment* 85, 429-440.

Maki, M., Nishida, K., Saigusa, N., Akiyama, T., 2005. Evaluation of the relationship between NDVI and LAI in cool-temperate deciduous forest, The Proceeding of Asian Conference of Remote Sensing.

Miller, J.R., White, H.P., Chen, J.M., Peddle, D.R., McDermid, G., Fournier, R.A., Shepherd, P., Rubinstein, I., Freemantle, J., Soffer, R., LeDrew, E., 1997. Seasonal change in understory reflectance of boreal forests and influence on canopy vegetation indices. *Journal of Geophysical Research: Atmospheres* 102(D24), 29475-29482.

Mustafa, Y.T., Van Laake, P.E., Stein, A., 2011. Bayesian network modeling for improving forest growth estimates. *IEEE Transactions on Geoscience and Remote Sensing*, 49(2), 639-649.

Myneni, R., Knyazikhin, Y., Glassy, J., Votava, P., Shabanov, N., 2003. User's Guide FPAR, LAI (ESDT: MOD15A2) 8-day Composite NASA MODIS Land Algorithm. http://cybele.bu.edu/modismisr/products/modis/userguide.pdf (accessed February 27, 2013).

Myneni, R.B., Hoffman, S., Knyazikhin, Y., Privette, J.L., Glassy, J., Tian, Y., Wang, Y., Song, X., Zhang, Y., Smith, G.R., Lotsch, A., Friedl, M., Morisette, J.T., Votava, P., Nemani, R.R., Running, S.W., 2002. Global products of vegetation leaf area and fraction absorbed PAR from year one of MODIS data. *Remote Sensing of Environment* 83(1–2), 214-231.

Ollinger, S.V., 2003. Forest ecosystems. http://www.els.net/WileyCDA/ElsArticle/refId-a0003190.html (accessed 5 February, 2013).

Pandya, M.R., Singh, R.P., Chaudhari, K.N., Bairagi, G.D., Sharma, R., Dadhwal, V.K., Parihar, J.S., 2006a. Leaf area index retrieval using IRS LISS-III sensor data and validation of the MODIS LAI product over central India. IEEE Transactions on Geoscience and Remote Sensing 44(7), 1858-1865.

Pandya, M.R., Singh, R.P., Chaudhari, K.N., Bairagi, G.D., Sharma, R., Dadhwal, V.K., Parihar, J.S., 2006b. Leaf area index retrieval using IRS LISS-III sensor data and validation of the MODIS LAI product over central India. IEEE Transactions on Geoscience and Remote Sensing, 44(7), 1858-1865.

Pardo-Iguzquiza, E., Atkinson, P.M., 2007. Modelling the semivariograms and cross-semivariograms required in downscaling cokriging by numerical convolution-deconvolution. *Computers & Geosciences* 33(10), 1273-1284.

Pardo-Iguzquiza, E., Atkinson, P.M., Chica-Olmo, M., 2010. DSCOKRI: A library of computer programs for downscaling cokriging in support of remote sensing applications. *Computers & Geosciences* 36(7), 881-894.

Pardo-Iguzquiza, E., Chica-Olmo, M., Atkinson, P.M., 2006. Downscaling cokriging for image sharpening. *Remote Sensing of Environment* 102(12), 86-98.

Pardo-Iguzquiza, E., Rodríguez-Galiano, V.F., Chica-Olmo, M., Atkinson, P.M., 2011. Image fusion by spatially adaptive filtering using downscaling cokriging. *ISPRS Journal of Photogrammetry and Remote Sensing* 66(3), 337-346.

Peng, G., Ruiliang, P., Biging, G.S., Larrieu, M.R., 2003. Estimation of forest leaf area index using vegetation indices derived from Hyperion hyperspectral data. Geoscience and Remote Sensing, IEEE Transactions on 41(6), 1355-1362.

Pouteau, R., Rambal, S., Ratte, J.-P., Gogé, F., Joffre, R., Winkel, T., 2011. Downscaling MODIS-derived maps using GIS and boosted regression trees: The case of frost occurrence over the arid Andean highlands of Bolivia. Remote Sensing of Environment 115(1), 117-129.

Propastin, P., Erasmi, S., 2010. A physically based approach to model LAI from MODIS 250 m data in a tropical region. International Journal of Applied Earth Observation and Geoinformation 12(1), 47-59.

Qi, J., Chehbouni, A., Huete, A.R., Kerr, Y.H., Sorooshian, S., 1994. A modified soil adjusted vegetation index. *Remote Sensing of Environment* 48(2), 119-126.

Rouse J.W., H.R.H., Schell J.A., Deering D.W., Harlan J.C., 1974. Monitoring the vernal advancement of retrogradation of natural vegetation. *NASA/GSFC*, MD.

Running, S.W., Baldocchi, D.D., Turner, D.P., Gower, S.T., Bakwin, P.S., Hibbard, K.A., 1999. A Global Terrestrial Monitoring Network Integrating Tower Fluxes, Flask Sampling, Ecosystem Modeling and EOS Satellite Data. Remote Sensing of Environment 70(1), 108-127.

Singh, S.P., 2010. Impact of forest degradation on carbon density in soil and vegetation of shorea robusta, Sal, forests in the part of siwalik hills of Dehradun, India, using geospatial techniques, Applied Earth Obsevation Department. ITC- Faculty of Geo-Information Science and Earth Observation, The Netherlands, pp. 1-85.

Song, C., 2013. Optical remote sensing of forest leaf area index and biomass. *Progress in Physical Geography* 37(1), 98-113.

Spanner, M.A., Pierce, L.L., Peterson, D.L., Running, S.W., 1990. Remote sensing of temperate coniferous forest leaf area index The influence of canopy closure, understory vegetation and background reflectance. *International Journal of Remote Sensing* 11(1), 95-111.

Spanner, M.A., Pierce, L.L., Peterson, D.L., Running, S.W., 1990(b). Remote sensing of temperate coniferous forest leaf area index: The influence of canopy closure, understory vegetation and background reflectance. *International Journal of Remote Sensing* 11, 95-111.

Spanner, M.A., Pierce, L.L., Running, S.W., Peterson, D.L., 1990(a). The seasonality of AVHRR data of temperate coniferous forests: Relationship with leaf area index. Remote Sensing of Environment 33(2), 97-112.

Stathopoulou, M., Cartalis, C., 2009. Downscaling AVHRR land surface temperatures for improved surface urban heat island intensity estimation. Remote Sensing of Environment 113(12), 2592-2605.

Studley, H., Weber, K.T., 2010. Comparison of image resampling techniques for satellite imagery, Assessing post-fire recovery of sagebrush steppe rangelands in southeastern Idaho. GIS Training and Research Center, Idaho, p. 185.

Tian, Y., Woodcock, C.E., Wang, Y., Privette, J.L., Shabanov, N.V., Zhou, L., Zhang, Y., Buermann, W., Dong, J., Veikkanen, B., HÃ¤me, T., Andersson, K., Ozdogan, M., Knyazikhin, Y., Myneni, R.B., 2002. Multiscale analysis and validation of the MODIS LAI product: I. Uncertainty assessment. *Remote Sensing of Environment* 83(3), 414-430.

Wade, T., Sommer , S., 2006. A to Z GIS. ESRI Press, Redlands.

Wang, Q., Adiku, S., Tenhunen, J., Granier, A., 2005. On the relationship of NDVI with leaf area index in a deciduous forest site. *Remote Sensing of Environment* 94(2), 244-255.

Wilhelm, W.W., Ruwe, K., Schlemmer, M.R., 2000. Comparison of three leaf area index meters in a corn canopy. *Crop Sciences*. 40(4), 1179-1183.

Wolf, P.R., Dewitt, B.A., 2004. Elements of photogrammetry with application in GIS, 3rd ed. McGraw-Hill, Singapore.

Woodcock, C.E., Strahler, A.H., 1987. The factor of scale in remote sensing. *Remote Sensing of Environment* 21(3), 311-332.

Zhan, W., Chen, Y., Zhou, J., Li, J., Liu, W., 2011. Sharpening Thermal Imageries: A Generalized Theoretical Framework From an Assimilation Perspective. *IEEE Transactions on Geoscience and Remote Sensing*, 49(2), 773-789.

Zurita-Milla, R., Kaiser, G., Clevers, J.G.P.W., Schneider, W., Schaepman, M.E., 2009. Downscaling time series of MERIS full resolution data to monitor vegetation seasonal dynamics. *Remote Sensing of Environment* 113(9), 1874-1885.

APPENDIX

Appendix 1: R-code to estimate variogram of LAI and NDVI and cross-variogram between LAI and NDVI

a) Reload package in R software

```
> require(gstat)
> require(raster)
> require(rgdal)
```

b) Display Image

```
> LAI_image <- raster("LAI.img")
> NDVI_image <- raster("NDVI.img")
```

c) Estimating variogram from LAI image

```
> M_LAI <- "LAI.img"
> dataset_LAI <- GDAL.open(M_LAI)
> dataset_LAI
> displayDataset(dataset_LAI, band=1, reset.par=FALSE)
> datatable_LAI <- getRasterTable(dataset_LAI, band = NULL, offset = c(0, 0),region.dim = dim(dataset_LAI))
> datatable_LAI_new <- datatable_LAI[!is.na(datatable_LAI[,3]),]
> datatable_LAI_new
> coordinates(datatable_LAI_new) <- ~x+y
> M_LAI.ev <- variogram(band1~1, data=datatable_LAI_new, cutoff=6000)
```

d) Estimating variogram from NDVI image

```
> M_NDVI <- "NDVI.img"
> dataset_NDVI <- GDAL.open(M_NDVI)
> dataset_NDVI
> displayDataset(dataset_NDVI, band=1, reset.par=FALSE)
> datatable_NDVI <- getRasterTable(dataset_NDVI, band = NULL, offset = c(0, 0),region.dim = dim(dataset_NDVI))
> datatable_NDVI_new <- datatable_NDVI[!is.na(datatable_NDVI[,3]),]
> datatable_NDVI_new
> coordinates(datatable_NDVI_new) <- ~x+y
> M_NDVI.ev <- variogram(band1~1, data=datatable_NDVI_new, cutoff=6000)
```

e) Estimating Cross-variogram

```
> g <- gstat(NULL, "M_LAI_250", band1~1, datatable_LAI_new_resample)
> g <- gstat(g, "M_NDVI_250", band1~1, datatable_NDVI_new)
> g
> cross.variogram <- variogram(g, cutoff=6000)
```